THE DARK ENERGY SURVEY

Cosmology with DES Year-1 data: from 3x2pt analyses to the CMB imprint of cosmic voids

Pauline Vielzeuf, SISSA

3rd World Summit on Exploring the Dark Side of the Universe.
March 9th 2020 , Pointe-à-Pitre Guadeloupe

ifpU

ma per seguir virtute e canoscenza
SISSA

Outline

- Overview of DES
- Probing cosmology with DESY1
  - DES individual probe results
  - Combination with other surveys
  - Beyond 3X2pts : additional probes
- DESY1 Cosmic voids imprint in the CMB radiation
  - Overview and methodology
  - Results

The Dark Energy Survey Camera

Imaging galaxy survey.

5000 sq. deg. after 6 years (2013-2019)

570-Megapixel digital camera, DECam, mounted on the Blanco 4-meter telescope at Cerro Tololo Inter-American Observatory (Chile).

Five filters are used (grizY) with a nominal limiting magnitude $i_{AB} \simeq 24$ and with a typical exposure time of 90 sec for griz and 45 sec for Y

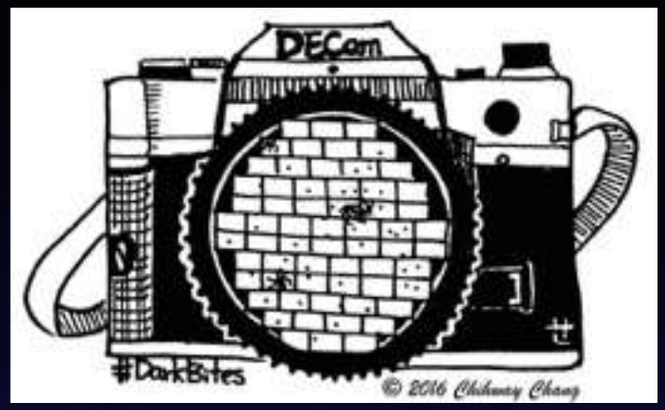

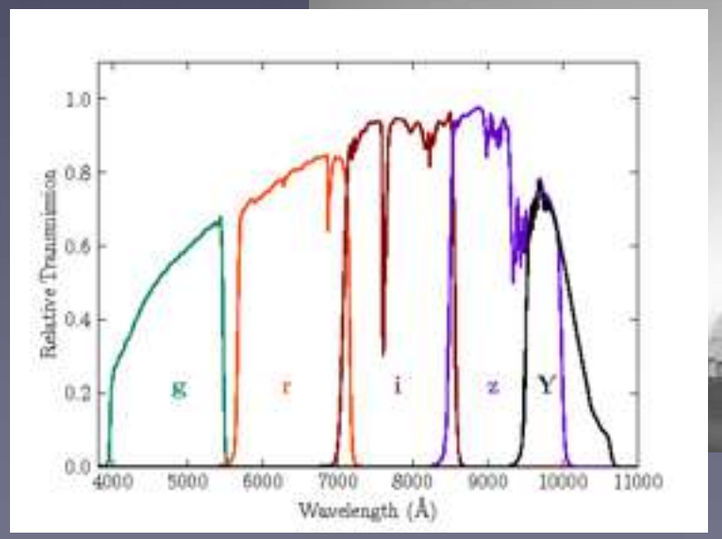

400 hundred scientists

7 countries

25 institutions

Credit: Judit Prat

THE DARK ENERGY SURVEY

DES footprint

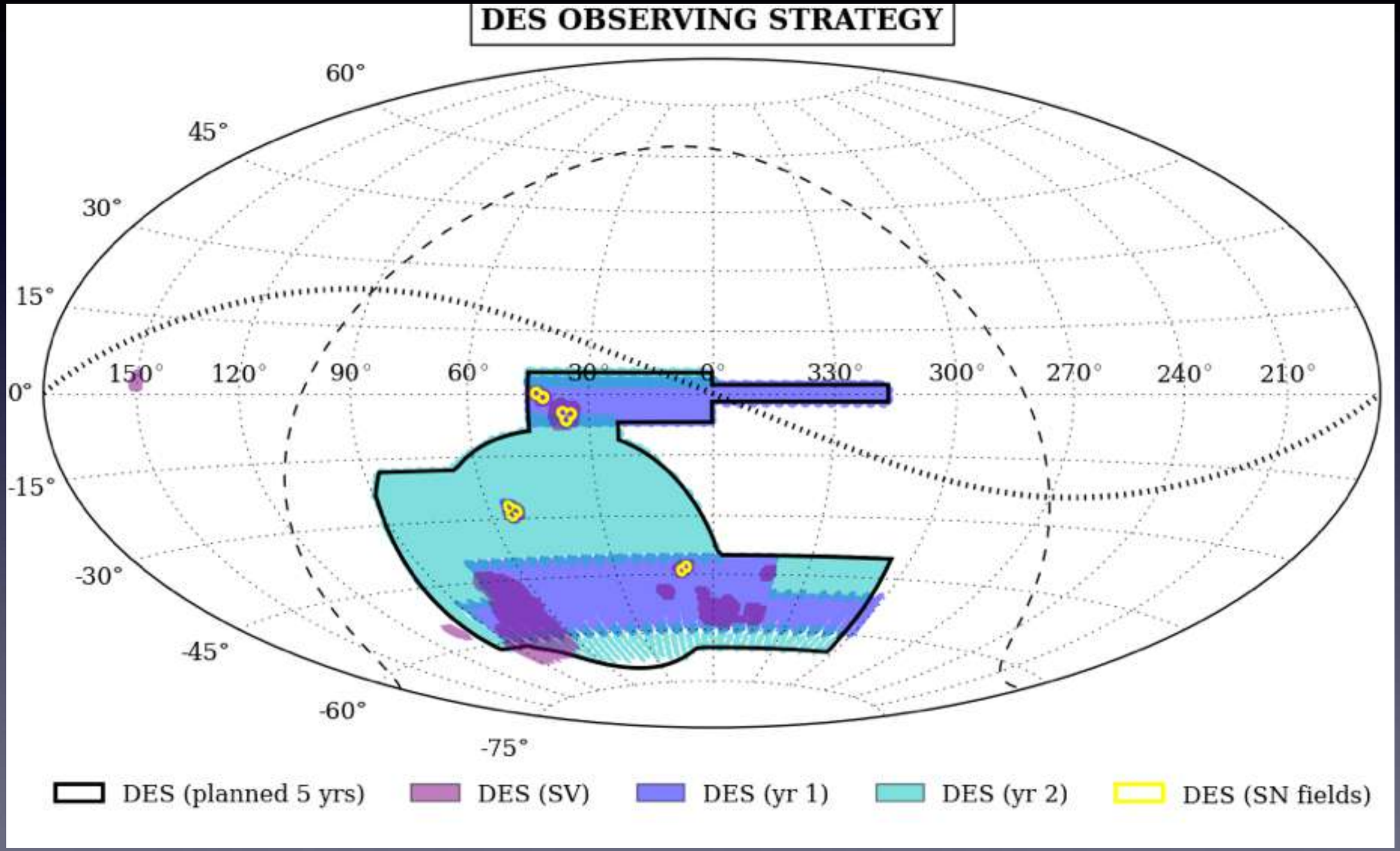

DESY1

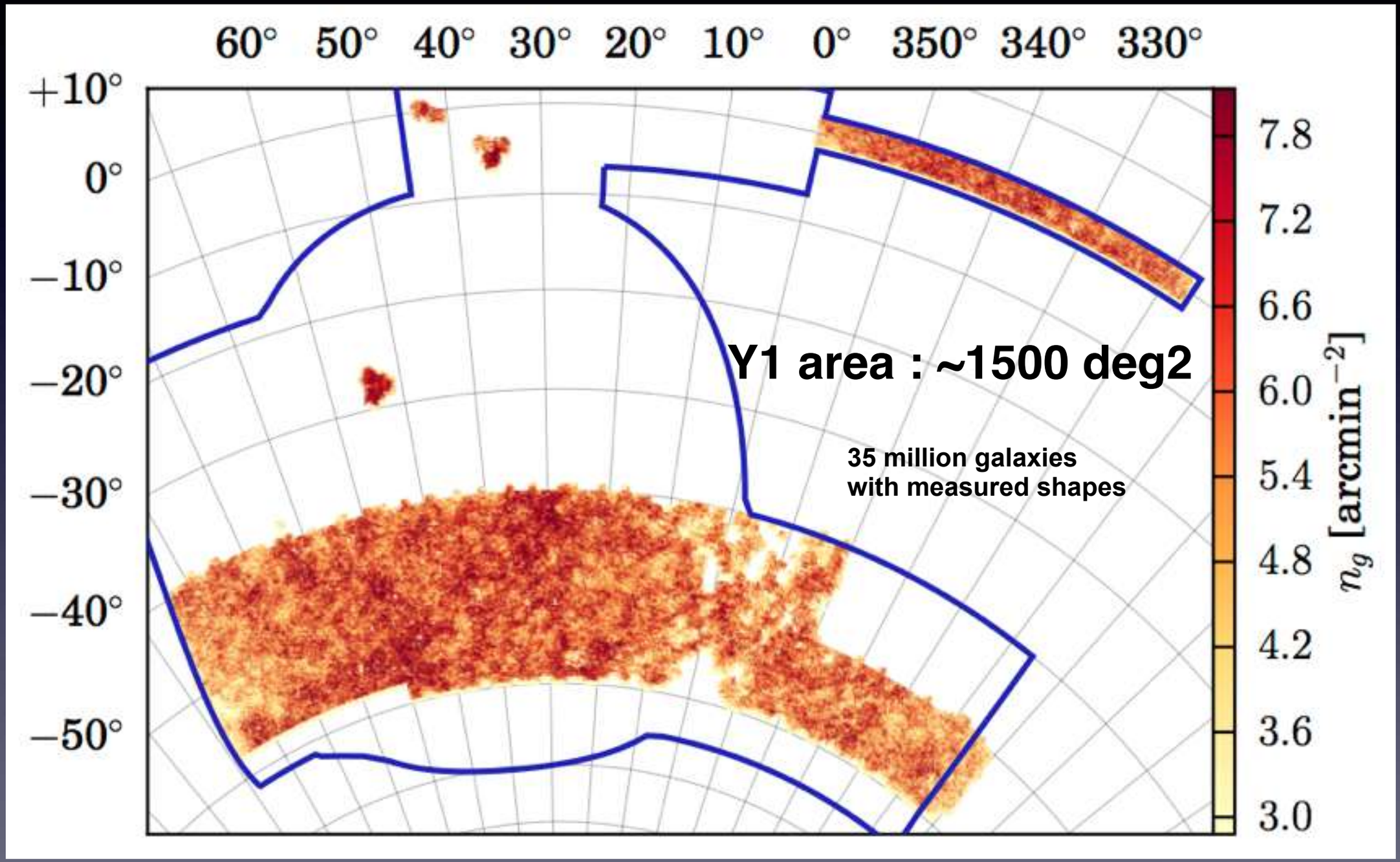
60° 50° 40° 30° 20° 10° 0° 350° 340° 330°
+10°
0°
−10°
−20°
−30°
−40°
−50°
Y1 area : ~1500 deg2
35 million galaxies
with measured shapes
7.8
7.2
6.6
6.0
5.4
4.8
4.2
3.6
3.0
n_g [arcmin^{-2}]

3 probes / 2 point statistics
=
3X2pt cosmological analysis

Galaxy Clustering

$$< \delta_g \delta_g >$$

Cosmic Shear

$$< \delta_\epsilon \delta_\epsilon >$$

Galaxy Galaxy lensing

$$< \delta_g \delta_\epsilon >$$

Galaxy-Galaxy correlation
correlations between galaxy **position** as a function of their separation

Shear-Shear correlation
correlations between galaxy **ellipticity** as a function of their separation

Galaxy-Shear correlation
correlations between the **ellipticity** of background galaxy with the **position** of foreground ones as a function of their separation

DESY1

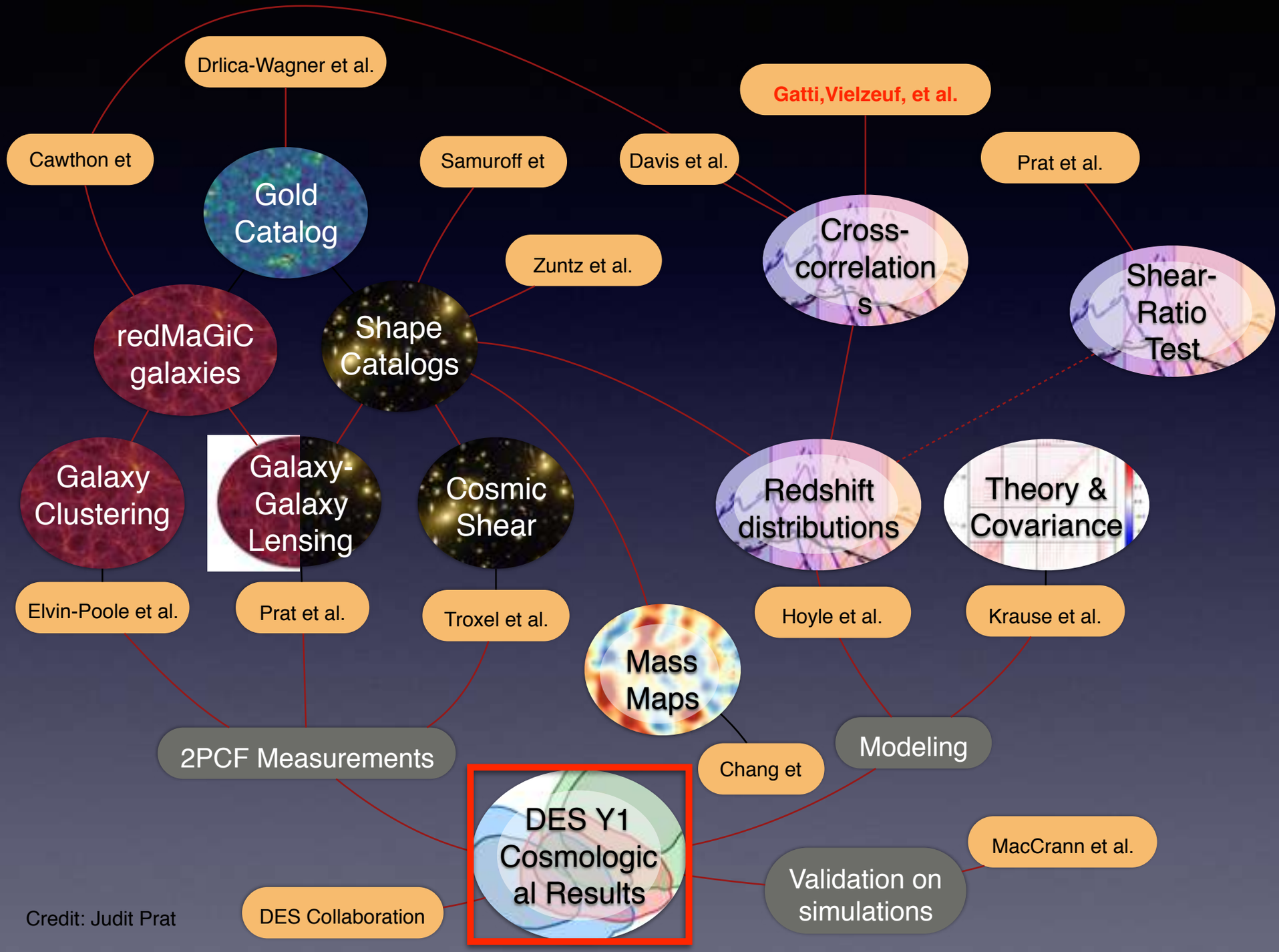
Drlica-Wagner et al.
Gatti,Vielzeuf, et al.
Cawthon et
Samuroff et
Davis et al.
Prat et al.
Gold Catalog
Zuntz et al.
Cross-correlations
Shear-Ratio Test
redMaGiC galaxies
Shape Catalogs
Galaxy Clustering
Galaxy-Galaxy Lensing
Cosmic Shear
Redshift distributions
Theory & Covariance
Elvin-Poole et al.
Prat et al.
Troxel et al.
Hoyle et al.
Krause et al.
Mass Maps
2PCF Measurements
Chang et
Modeling
DES Y1 Cosmological Results
MacCrann et al.
Validation on simulations
DES Collaboration
Credit: Judit Prat

The samples of DESY1

redMaGiC (Rozo et al. (2016)): algorithm that select Luminous Red Galaxies

z range	$L_{\rm min}/L_*$	$n_{\rm gal}$ (deg^{-2})	$N_{\rm gal}$
$0.15 < z < 0.3$	0.5	0.0134	63719
$0.3 < z < 0.45$	0.5	0.0344	163446
$0.45 < z < 0.6$	0.5	0.0511	240727
$0.6 < z < 0.75$	1.0	0.0303	143524
$0.75 < z < 0.9$	1.5	0.0089	42275

Bin	Extent	$n_{\rm eff}$	
		C13	H12
Full	0.20 – 1.30	5.14	5.50
1	0.20 – 0.43	1.47	1.52
2	0.43 – 0.63	1.46	1.55
3	0.63 – 0.90	1.50	1.63
4	0.90 – 1.30	0.73	0.83

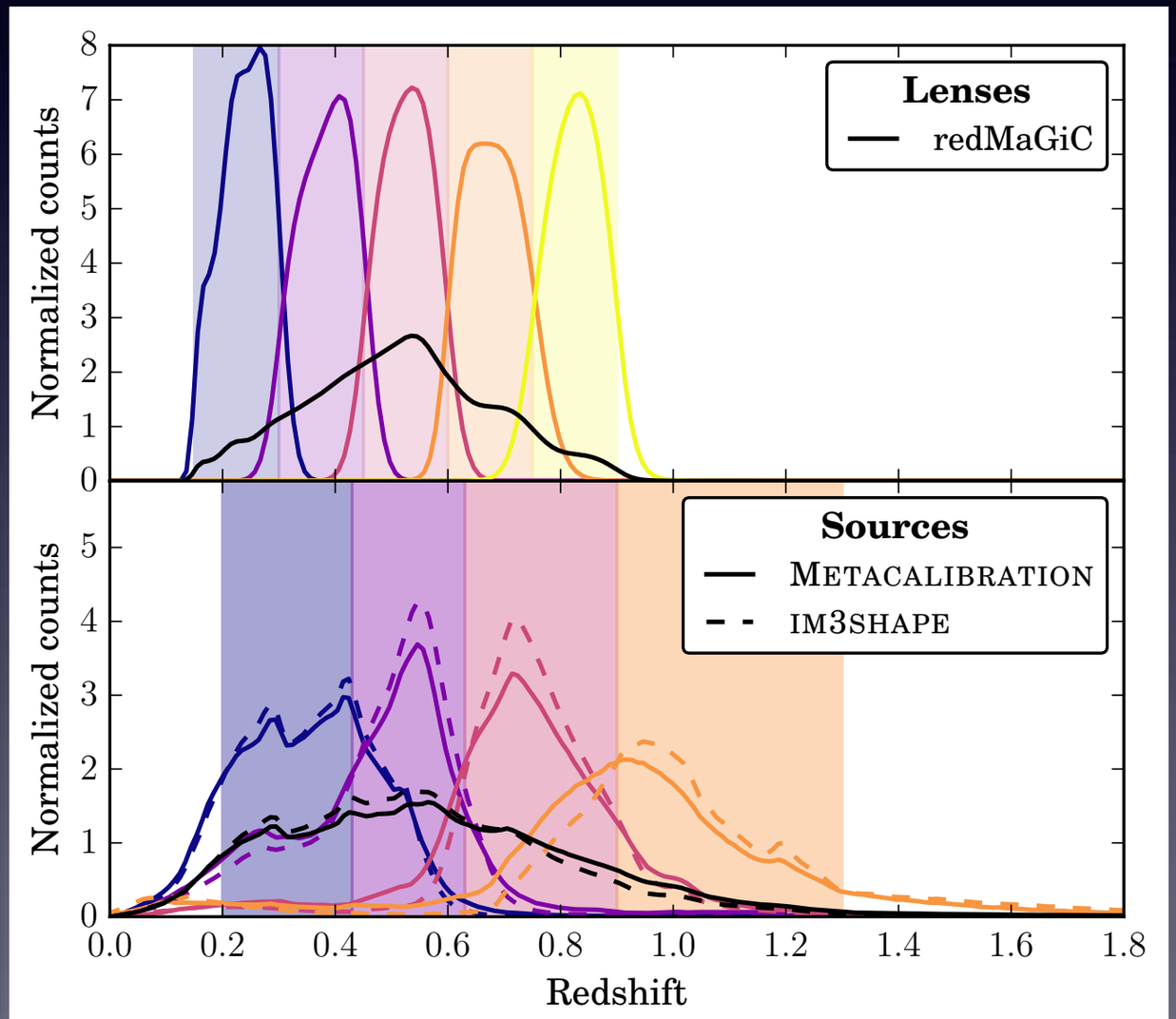

THE DARK ENERGY SURVEY

DES Y1 Results

Cosmic Shear

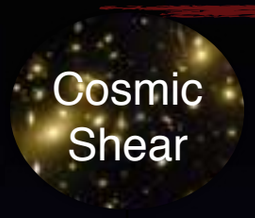

Troxel et al.

$$\propto \Omega_m^2 \sigma_8^2$$

Estimator

$$\hat{\xi}^{ij}_{\pm}(\theta) = \frac{\sum_{ab} W_a W_b \left[\hat{e}^i_{a,t}(\vec{\theta})\hat{e}^j_{b,t}(\vec{\theta}) \pm \hat{e}^i_{a,\times}(\vec{\theta})\hat{e}^j_{b,\times}(\vec{\theta})\right]}{\sum_{ab} W_a W_b S_a S_b}$$

Model

$$\xi^{ij}_{+/-}(\theta) = (1+m^i)(1+m^j)\int \frac{dl\, l}{2\pi} J_{0/4}(l\theta) \int d\chi \times \frac{q^i_s(\chi) q^j_s(\chi)}{\chi^2} P_{\rm NL}\left(\frac{l+1/2}{\chi}, z(\chi)\right) \quad (\Gamma$$

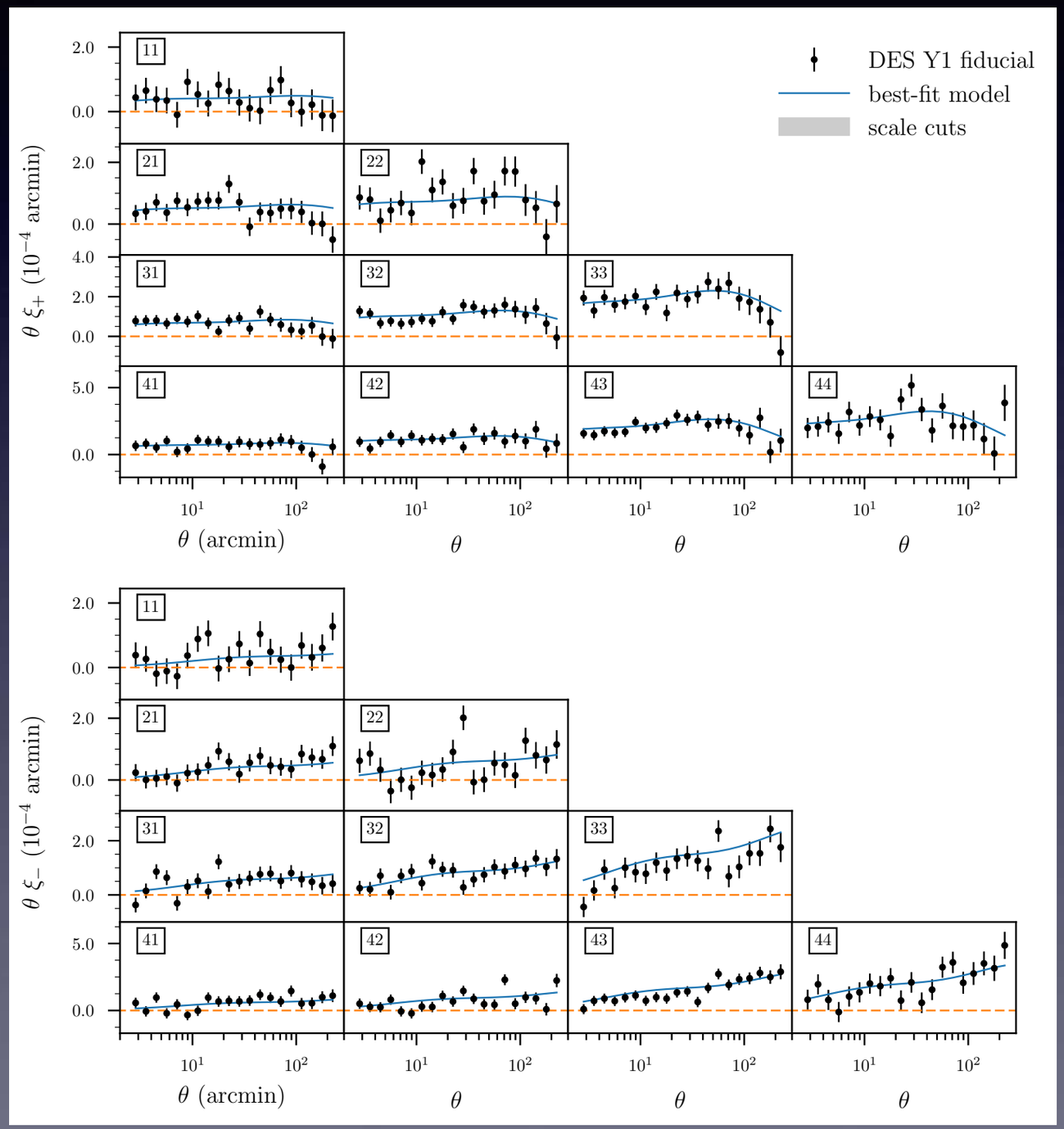

DES Y1 Results

Galaxy Clustering

$$\propto b^2\sigma_8^2$$

Elvin-Poole et al.

Galaxy Clustering

Estimator

$$\hat{w}(\theta) = \frac{DD - 2DR + RR}{RR},$$

model

$$w^i(\theta) = \left(b^i\right)^2 \int \frac{dl\, l}{2\pi} J_0(l\theta) \int d\chi \times \frac{\left[n_1^i(z(\chi)\right]^2}{\chi^2 H(z)} P_{\rm NL}\left(\frac{l+1/2}{\chi}, z(\chi)\right)$$

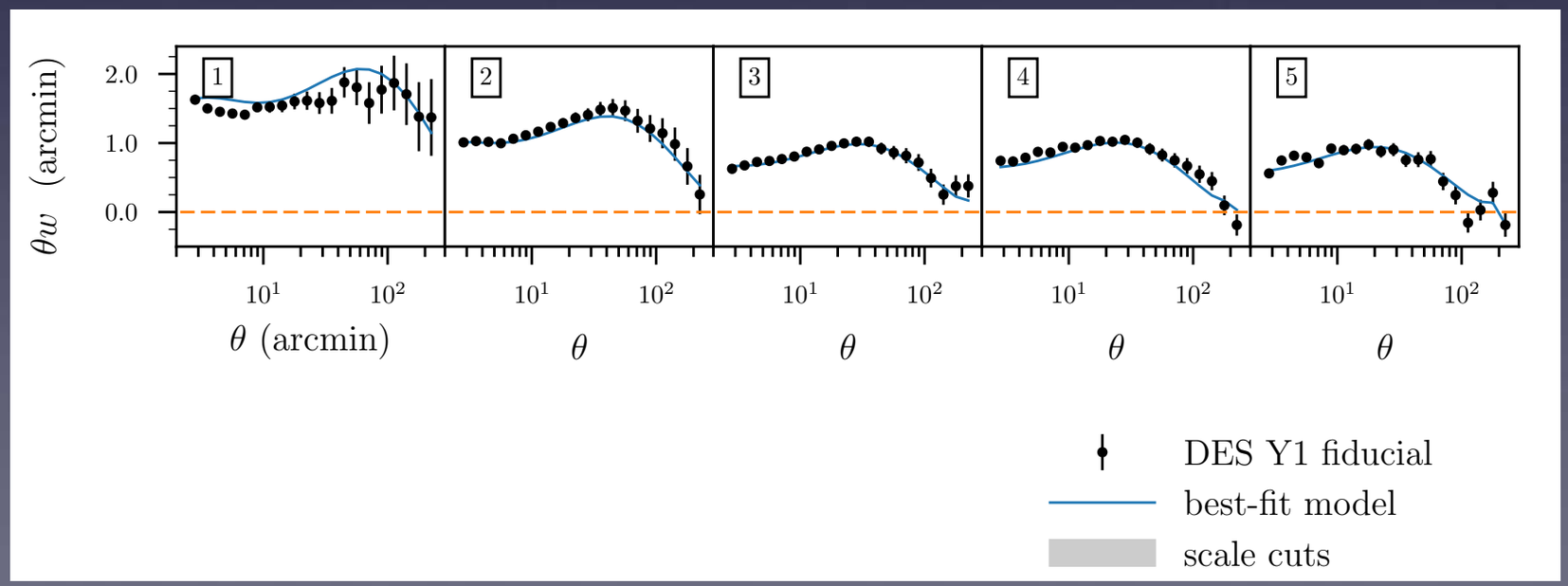

THE DARK ENERGY SURVEY

DES Y1 Results

Galaxy Galaxy Lensing

Galaxy-Galaxy Lensing

$$\propto b\Omega_m\sigma_8^2$$

Prat et al.

Model

$$\gamma_{\rm t}^{ij}(\theta) = b^i(1+m^j)\int \frac{dl\, l}{2\pi} J_2(l\theta) \int d\chi n_{\rm l}^i(z(\chi)) \times \frac{q_s^j(\chi)}{H(z)\chi^2} P_{\rm NL}\left(\frac{l+1/2}{\chi}, z(\chi)\right), \quad ($$

Estimator

$$\langle \gamma_\alpha(\theta)\rangle = \frac{\sum_j \omega_j e_{\alpha,j}}{\sum_j \omega_j},$$

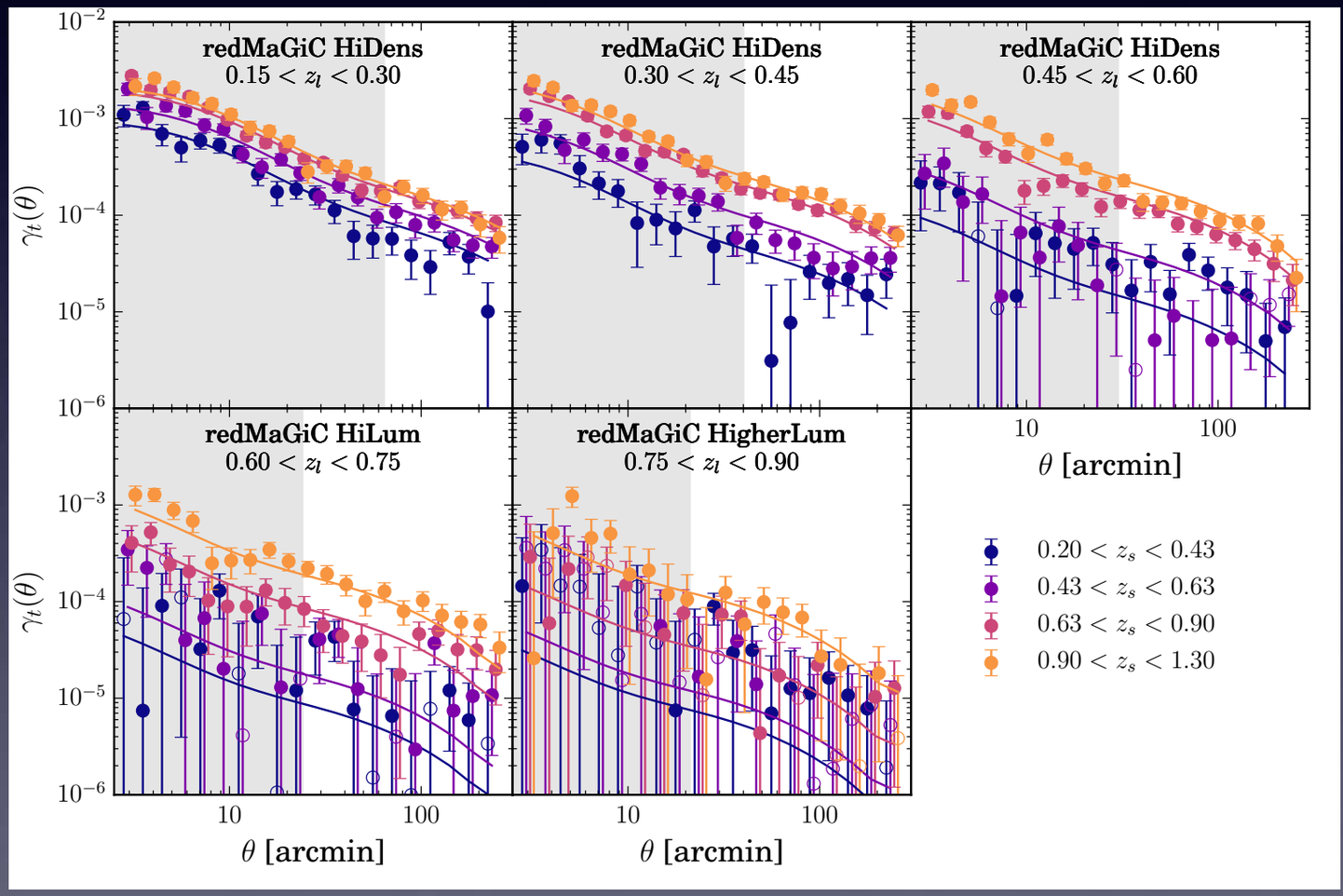

THE DARK ENERGY SURVEY

DES Y1 Results

Cosmic Shear (only)

DES Y1 Cosmological Results

DES Collaboration

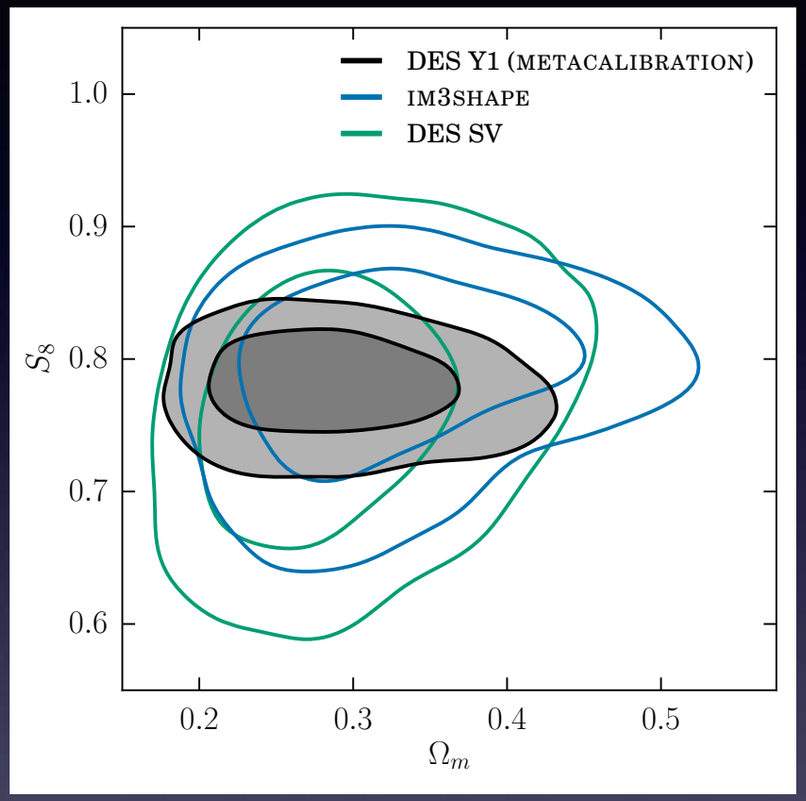

$$S_8 = 0.782^{+0.027}_{-0.027}$$ 68% CI

(3 times better than SV)

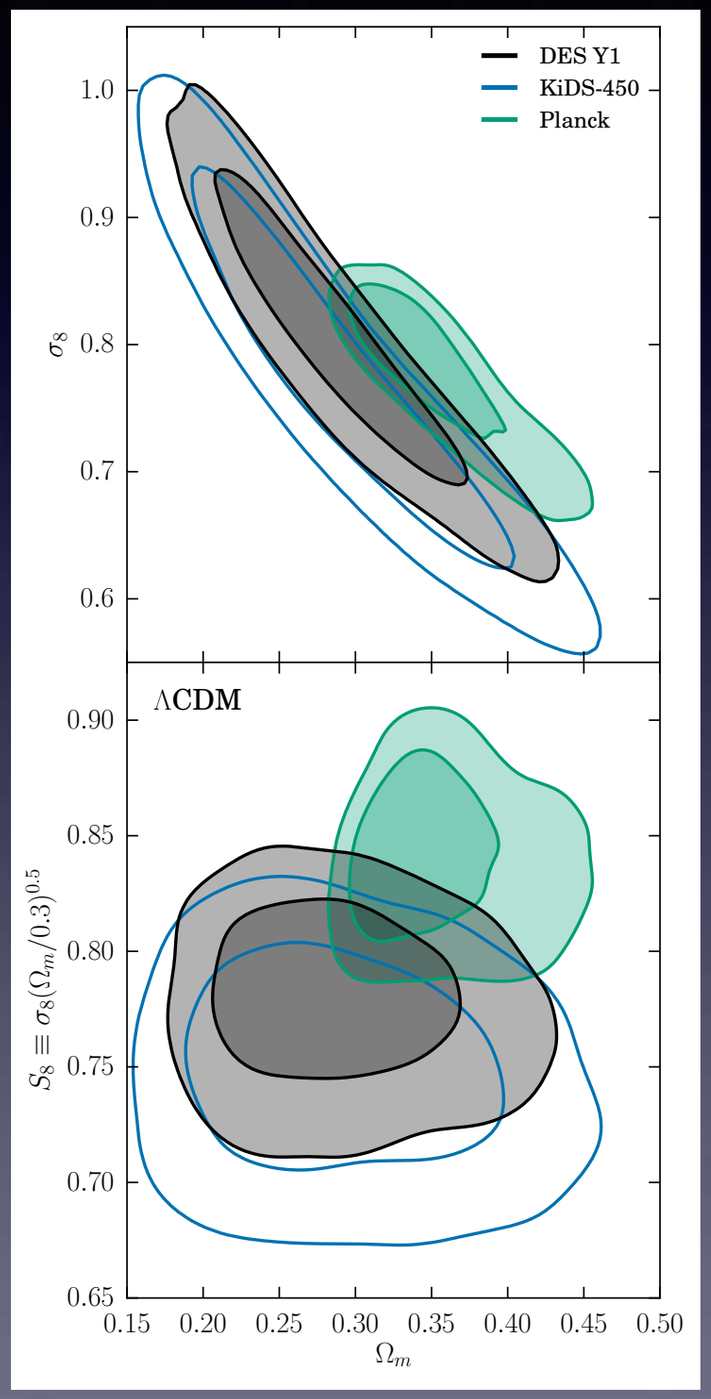

THE DARK ENERGY SURVEY

Combined Results : 3X2pt

consistent cosmological results from these three two-point functions and from their combination

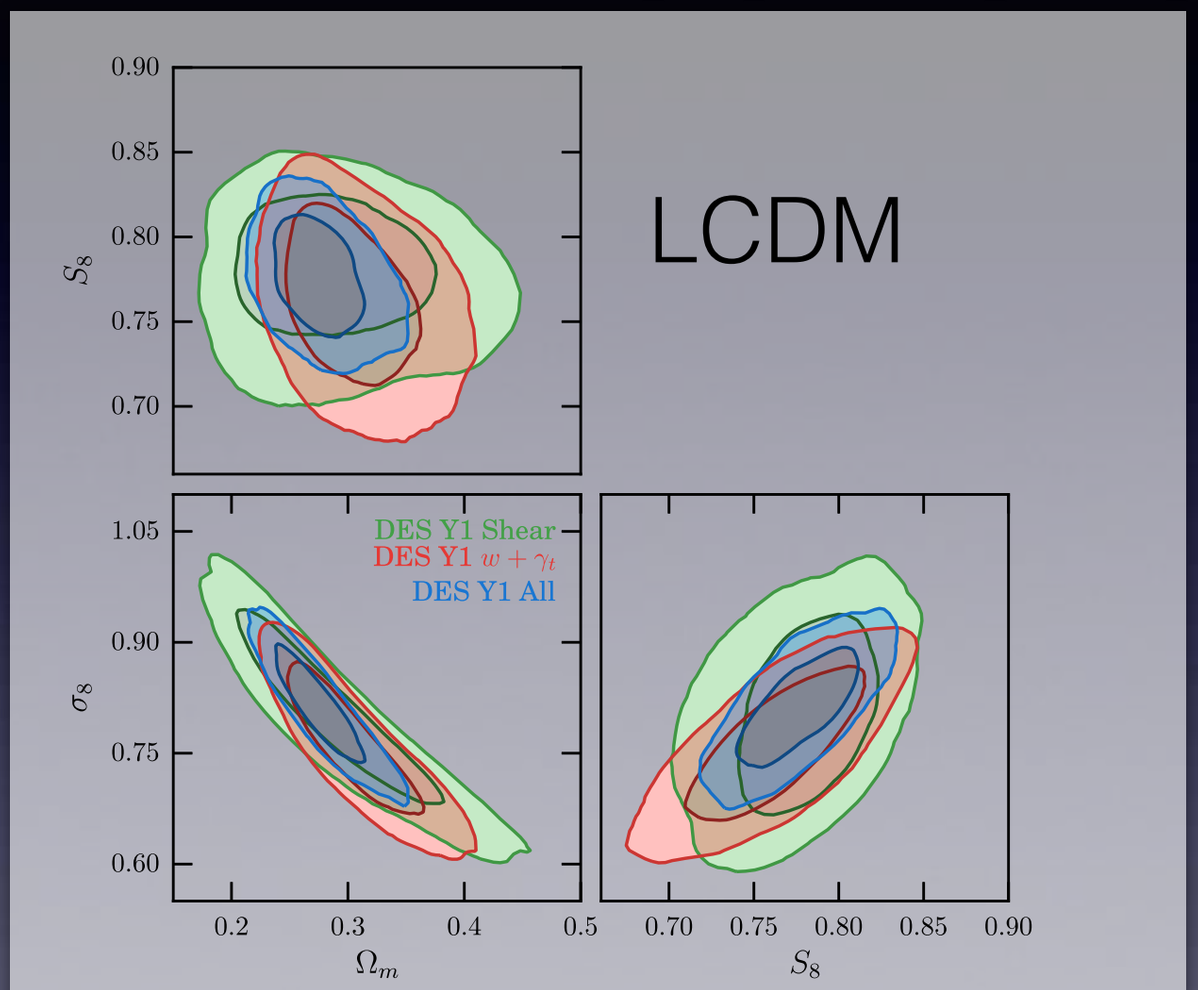

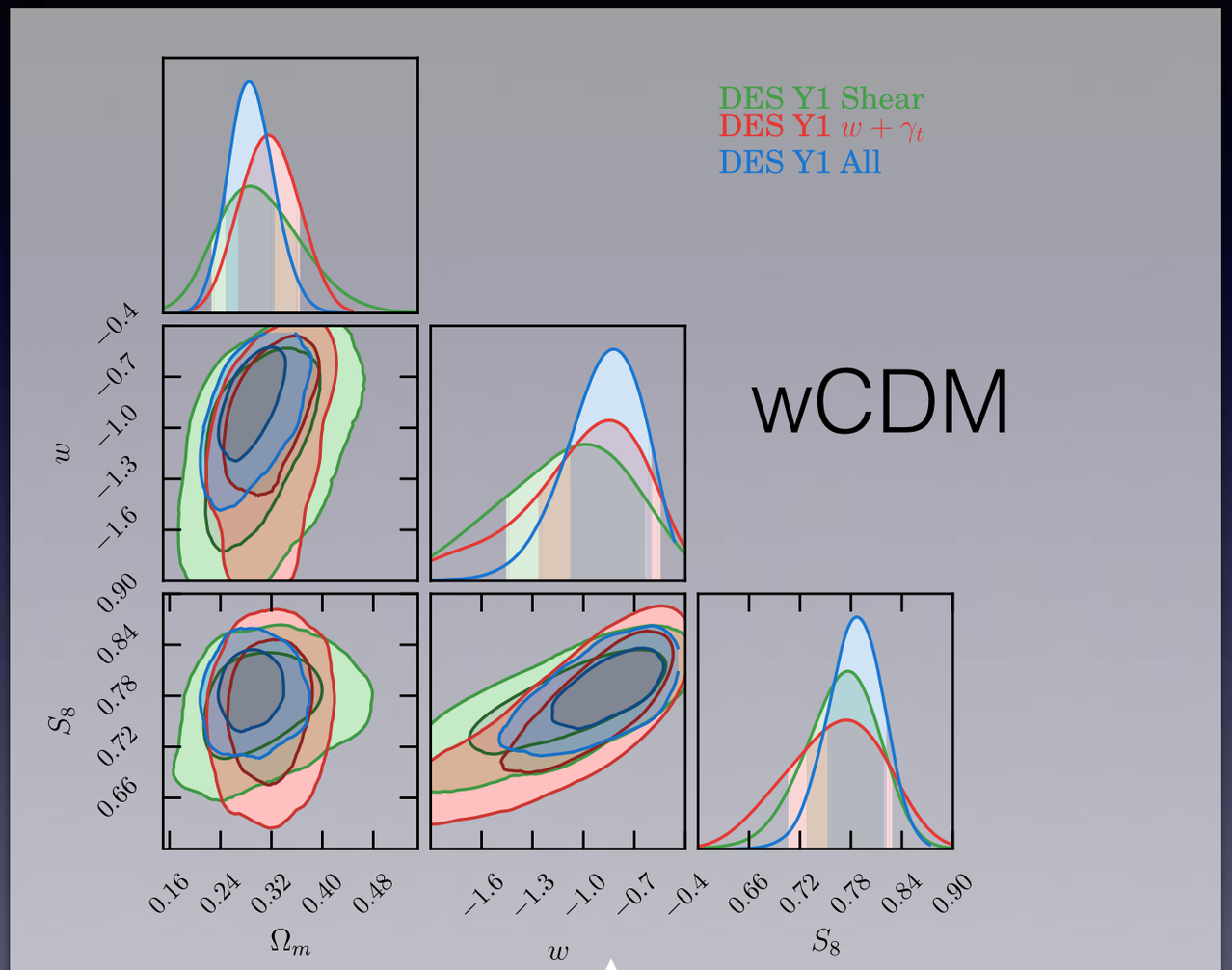

Agreement between lensing and clustering

Model	Data Sets	Ω_m	S_8
ΛCDM	DES Y1 $\xi_{\pm}(\theta)$	$0.323^{+0.048}_{-0.069}$	$0.791^{+0.019}_{-0.029}$
ΛCDM	DES Y1 $w(\theta) + \gamma_t$	$0.293^{+0.043}_{-0.033}$	$0.770^{+0.035}_{-0.030}$
ΛCDM	DES Y1 3x2	$0.264^{+0.032}_{-0.019}$	$0.783^{+0.021}_{-0.025}$

No evidence of wCDM model

Model	Data Sets	Ω_m	S_8	w
wCDM	DES Y1 $\xi_{\pm}(\theta)$	$0.317^{+0.074}_{-0.054}$	$0.789^{+0.036}_{-0.038}$	$-0.82^{+0.26}_{-0.47}$
wCDM	DES Y1 $w(\theta) + \gamma_t$	$0.317^{+0.045}_{-0.041}$	$0.788^{+0.039}_{-0.067}$	$-0.76^{+0.19}_{-0.45}$
wCDM	DES Y1 3x2	$0.279^{+0.043}_{-0.022}$	$0.794^{+0.029}_{-0.027}$	$-0.80^{+0.20}_{-0.22}$

DES Y1 constraints rivals that from the Planck cosmic microwave background measurements

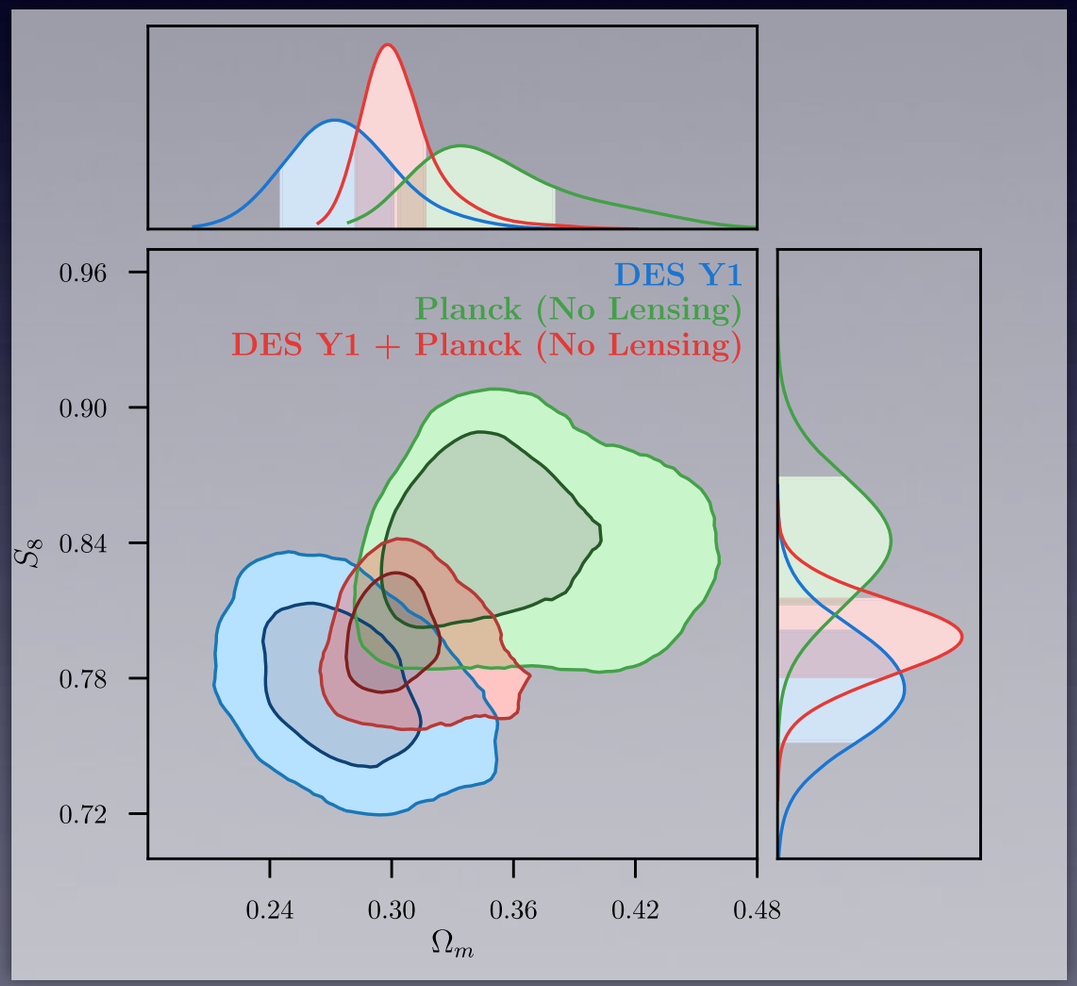

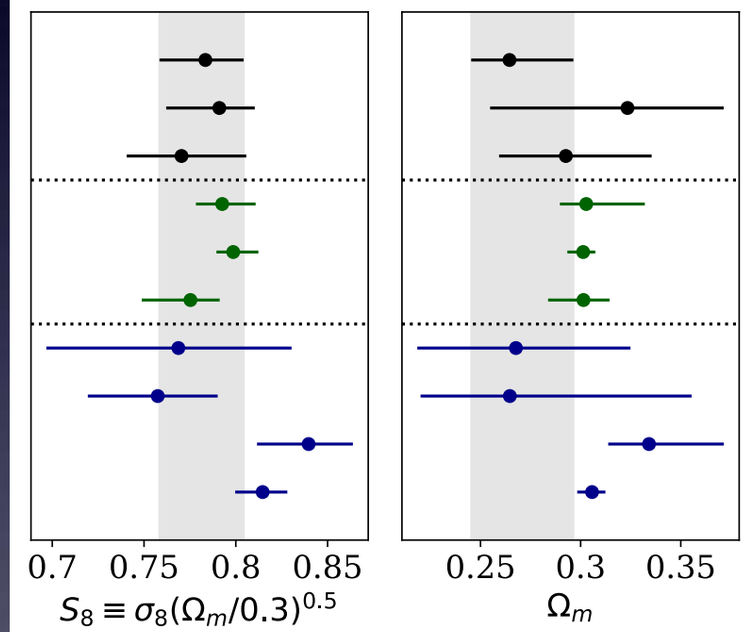

THE DARK ENERGY SURVEY

Going further
6X2pt

Dark Energy Survey Year 1 Results: Joint Analysis of Galaxy Clustering, Galaxy Lensing, and CMB Lensing Two-point Functions

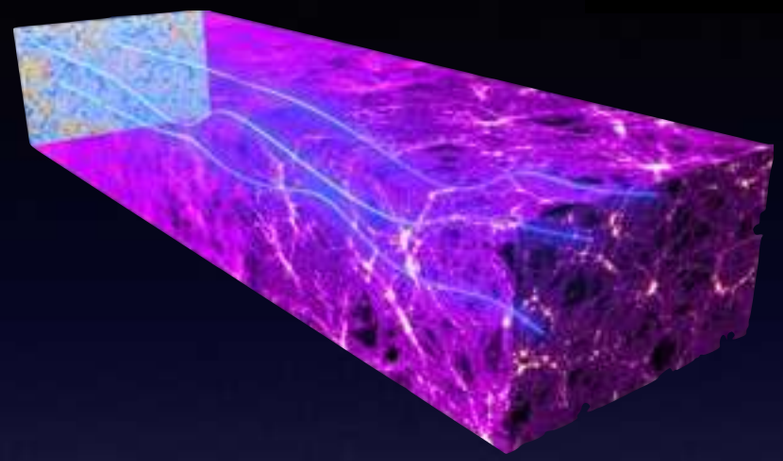

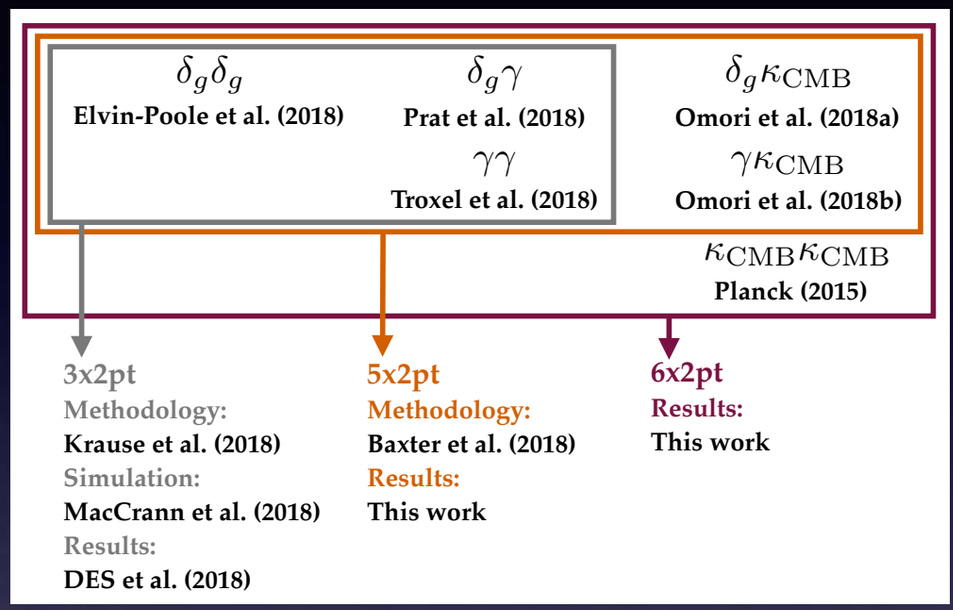

Some advantages:

- No source photo-z
- No intrinsic alignments
- No source blending
- High redshift sensitivity
- Independent test of
- galaxy lensing measurements

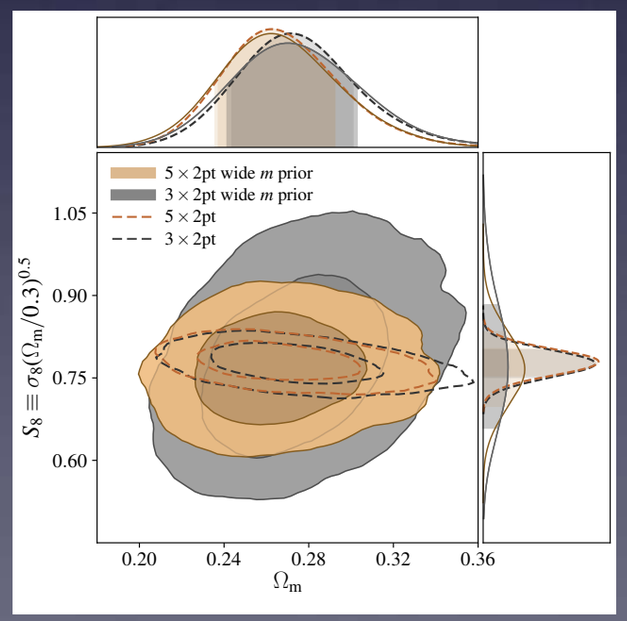

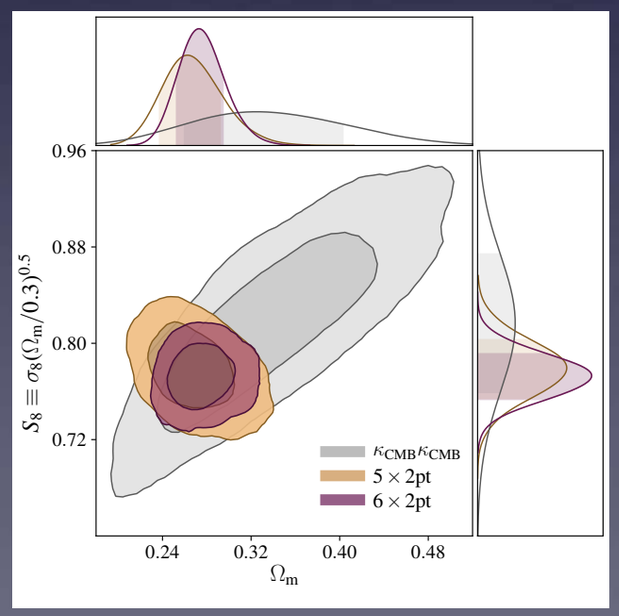

THE DARK ENERGY SURVEY

Clusters abundances

Dark Energy Survey Year 1 Results: Cosmological Constraints from Cluster Abundances and Weak Lensing

'arising from the highest peaks of the matter density field, their abundance and spatial distribution are sensitive to the growth of structures and cosmic expansion'

$$\sigma_8(\Omega_{\rm m}/0.3)^{\alpha}$$

Model

$$\langle N\rangle = \int_0^{\infty} dz^{\rm true} \int_{z_{\rm min}}^{z_{\rm max}} dz^{\rm ob} \int_{\lambda_{\rm min}}^{\lambda_{\rm max}} d\lambda^{\rm ob} \langle n|\lambda^{\rm ob}, z^{\rm true}\rangle \frac{dV}{dz^{\rm true}} P(z^{\rm ob}|z^{\rm true})$$

$$\langle M\rangle = \frac{1}{\langle N\rangle} \int_0^{\infty} dz^{\rm true} \int_{z_{\rm min}}^{z_{\rm max}} dz^{\rm ob} \int_{\lambda_{\rm min}}^{\lambda_{\rm max}} d\lambda^{\rm ob} \langle nM|\lambda^{\rm ob}, z^{\rm true}\rangle \frac{dV}{dz^{\rm true}} P(z^{\rm ob}|z^{\rm true}).$$

Measurement

Data vector is the DES Y1 redMaPPer cluster counts and weak-lensing masses.

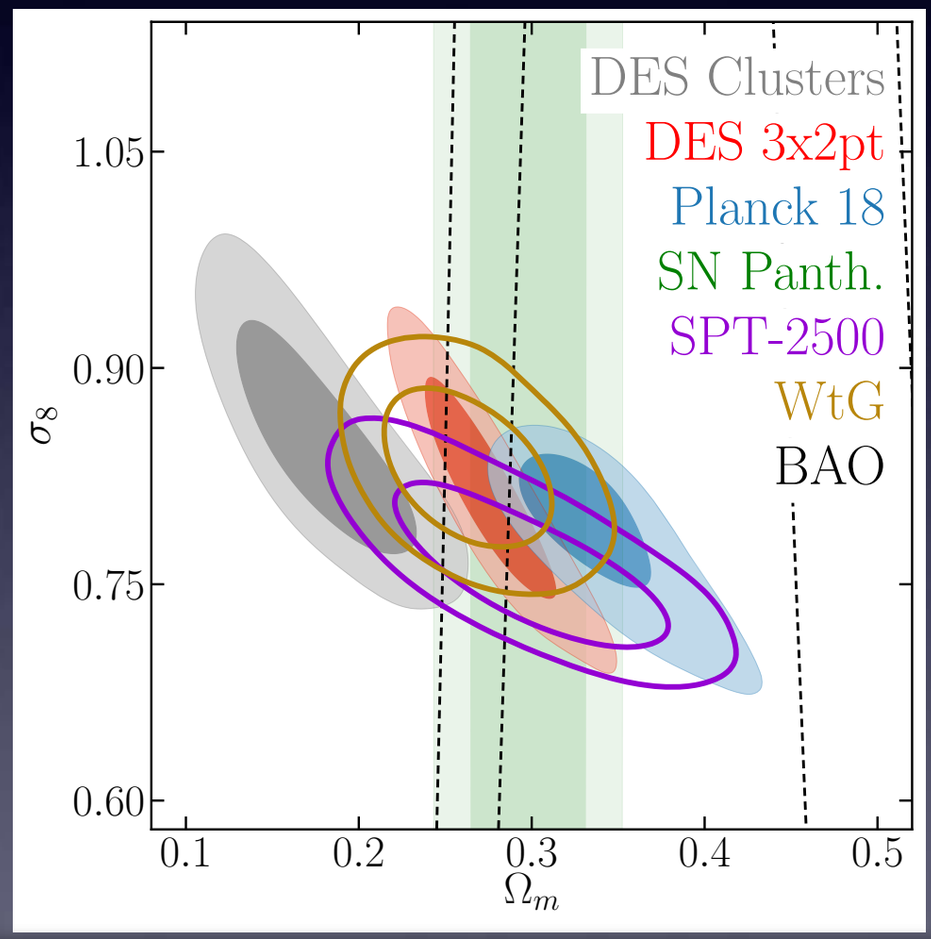

$\sigma_8 - \Omega_{\rm m}$ posteriors in 2.4σ tension with the DES Y1

5.6σ with the *Planck* CMB analysis.

Cosmic Voids in Y1

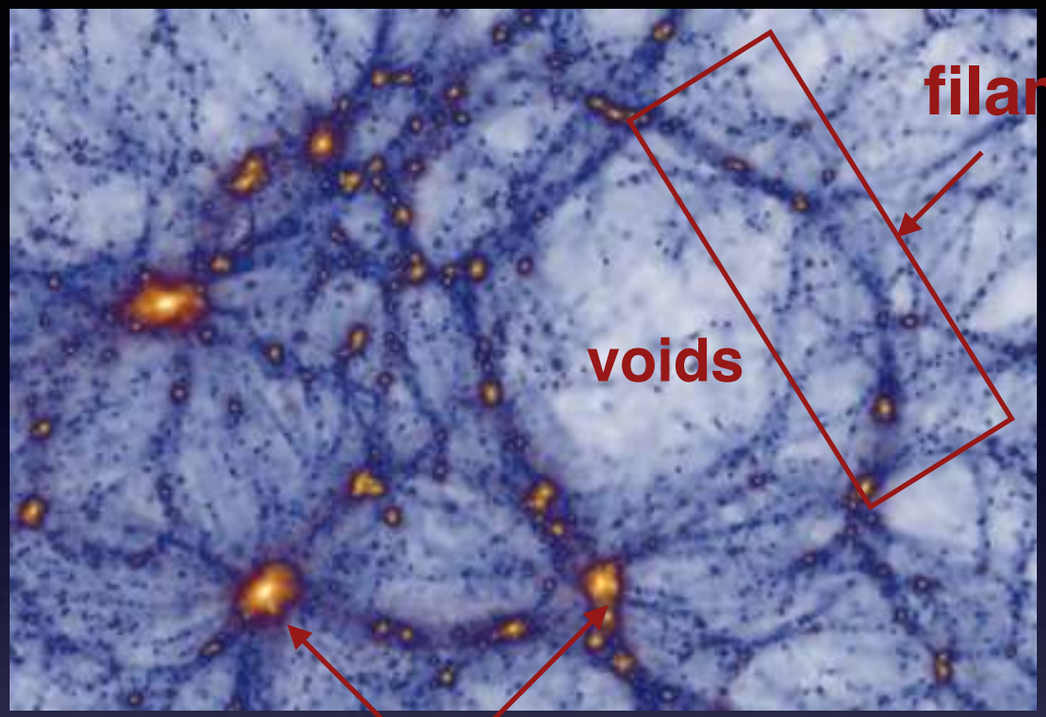

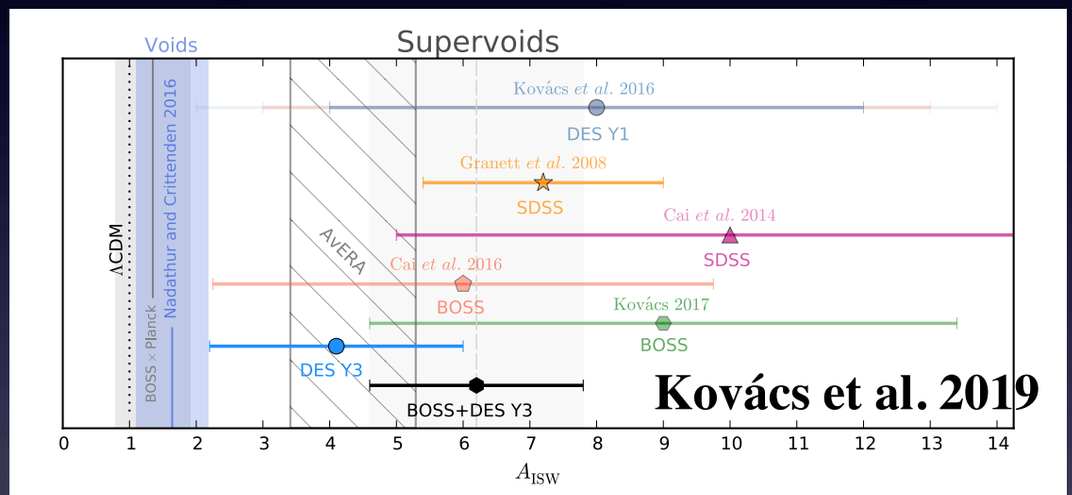

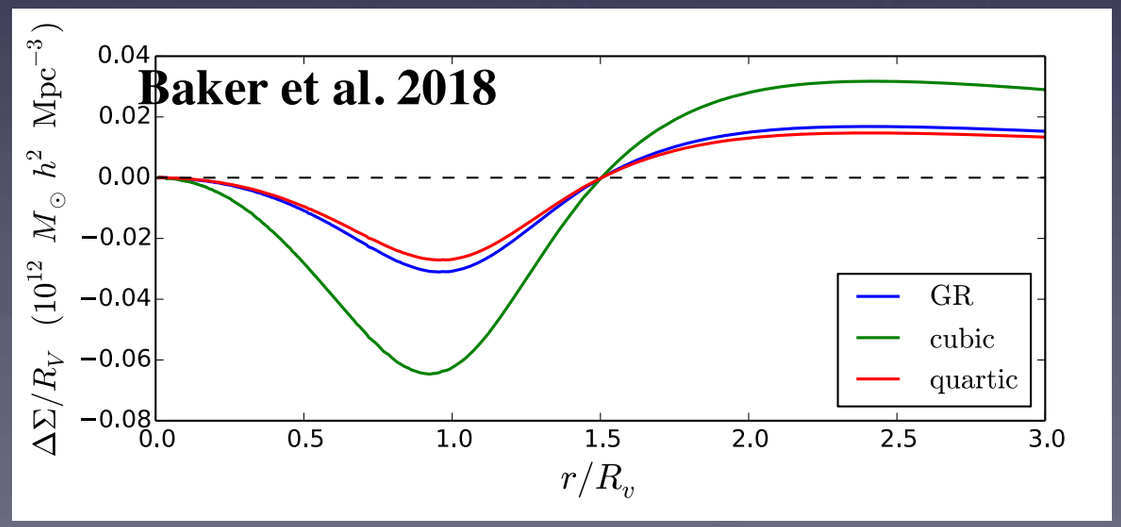

DES Y1 xPlanck

Dark Energy Survey Year 1 Results: the lensing imprint of cosmic voids on the Cosmic Microwave Background

P. Vielzeuf[1,2,3⋆] A. Kovács[1,4,5†], U. Demirbozan[1], P. Fosalba[6,7], E. Baxter[8], N. Hamaus[9], D. Huterer[10], R. Miquel[11,1], S. Nadathur[12], G. Pollina[9], C. Sánchez[8], L. Whiteway[13], T. M. C. Abbott[14], S. Allam[15], J. Annis[15], S. Avila[16], D. Brooks[13], D. L. Burke[17,18], A. Carnero Rosell[19,20], M. Carrasco Kind[21,22], J. Carretero[1], R. Cawthon[23], M. Costanzi[24,25], L. N. da Costa[20,26], J. De Vicente[19], S. Desai[27], H. T. Diehl[15], P. Doel[13], T. F. Eifler[28,29], S. Everett[30], B. Flaugher[15], J. Frieman[15,31], J. García-Bellido[16], E. Gaztanaga[6,7], D. W. Gerdes[32,10], D. Gruen[33,17,18], R. A. Gruendl[21,22], J. Gschwend[20,26], G. Gutierrez[15], W. G. Hartley[13,34], D. L. Hollowood[30], K. Honscheid[35,36], D. J. James[37], K. Kuehn[38,39], N. Kuropatkin[15], O. Lahav[13], M. Lima[40,20], M. A. G. Maia[20,26], M. March[8], J. L. Marshall[41], P. Melchior[42], F. Menanteau[21,22], A. Palmese[15,31], F. Paz-Chinchón[21,22], A. A. Plazas[42], E. Sanchez[19], V. Scarpine[15], S. Serrano[6,7], I. Sevilla-Noarbe[19], M. Smith[43], E. Suchyta[44], G. Tarle[10], D. Thomas[12], J. Weller[45,46,9], J. Zuntz[47]

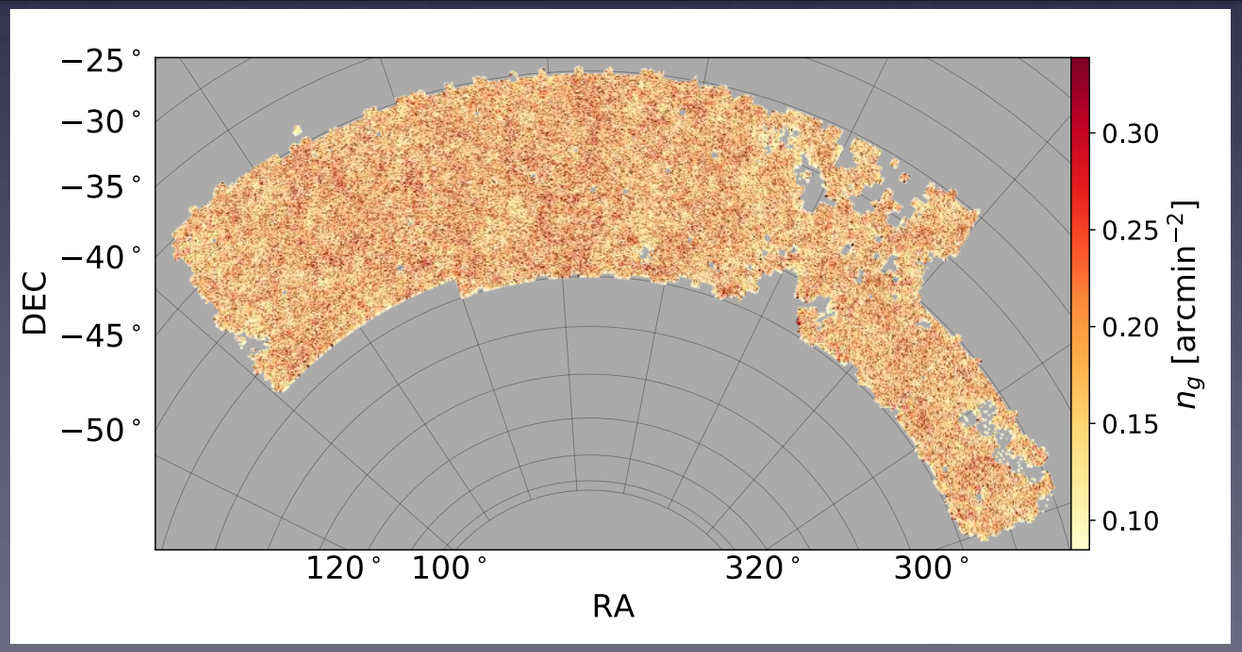

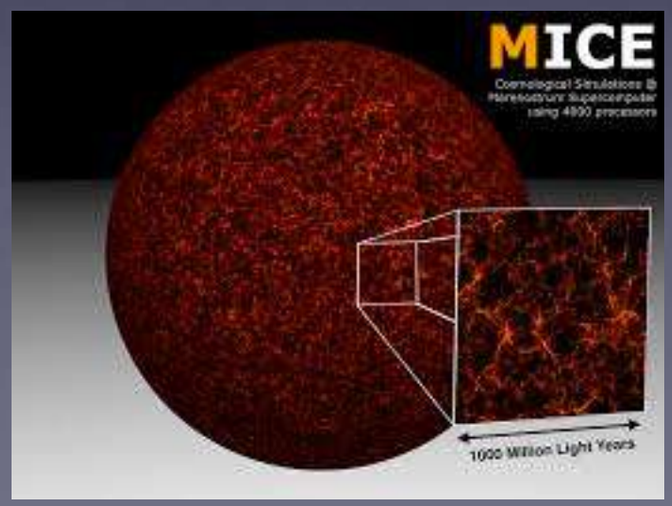

Void finder

- **Divide the sample in redshift slices. 100*Mpc/h* slices are shown to be a good compromise considering *redMaGiC* redshift accuracy.**

- **Compute the density field for each slice by counting the galaxy number in each pixel and smoothing the field with a Gaussian with a predefined smoothing scale.**

- **Select the most underdense pixel and grow around it the void until it reaches the mean density.**

- **Save the void, erase it from the density map and iterate the process with the following underdense pixel.**

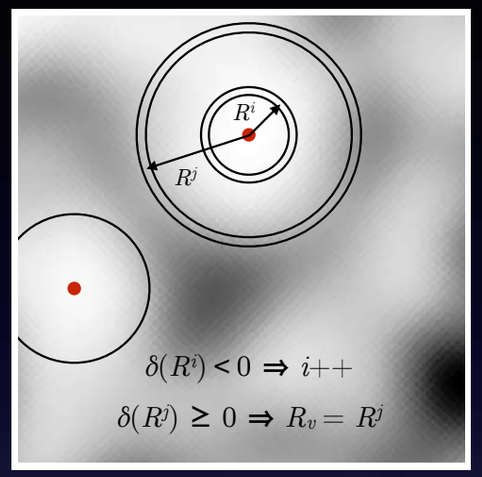

Figure 1. Graphical description of the void-finding algorithm presented in this paper. The background gray-scaled field is the smoothed galaxy field ($\sigma = 10$ Mpc/h) in a redshift slice used by the void-finder. The two solid (red) dots show two void centers. For the upper void, we show a circular shell or radius R^i. Since the density contrast $\delta(R^i) < 0$, the algorithm checks larger shells, up to radius R^j such that $\delta(R^j) \geqslant 0$. The void radius is then defined as $R_v = R^j$.

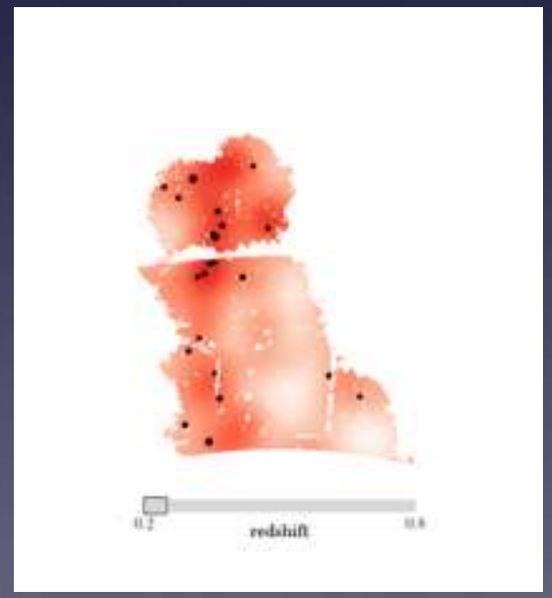

Sánchez et al. (DES Collaboration), MNRAS 465, 746, 2017.

Catalogs

Two tracers :
- **RedMagiC High-luminosity sample**
- **RedMagiC High-density sample**

Two smoothing scales:
10 Mpc/h
20 Mpc/h

4 void catalogs

smoothing scale 20Mpc/h

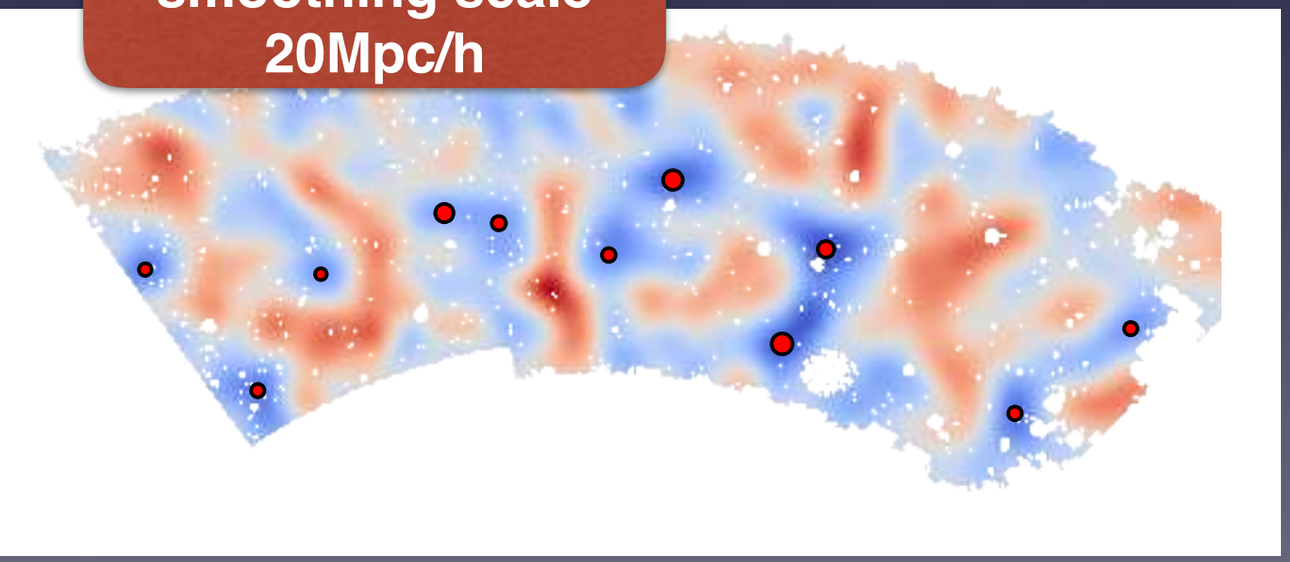

smoothing scale 10Mpc/h

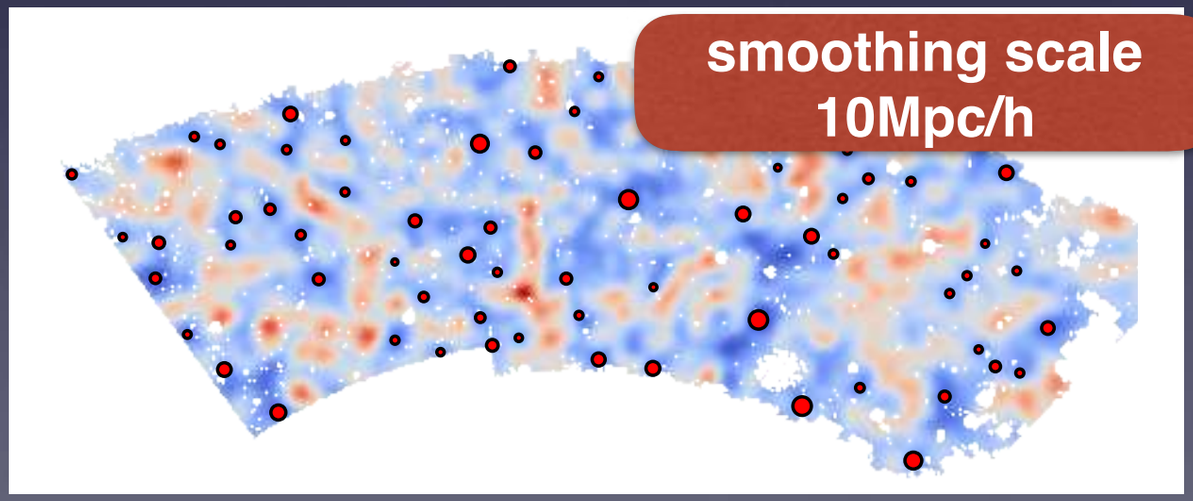

Catalogs

High luminosity (HL)

Smoothing	DES Y1	MICE 1	MICE 2
10 Mpc/h	1218	1158	1219
20 Mpc/h	411	364	400

High density (HD)

Smoothing	DES Y1	MICE 1	MICE 2
10 Mpc/h	518	521	495
20 Mpc/h	122	85	106

VIDE	DES Y1	MICE
All	7383	36115
Pruned	239	1687

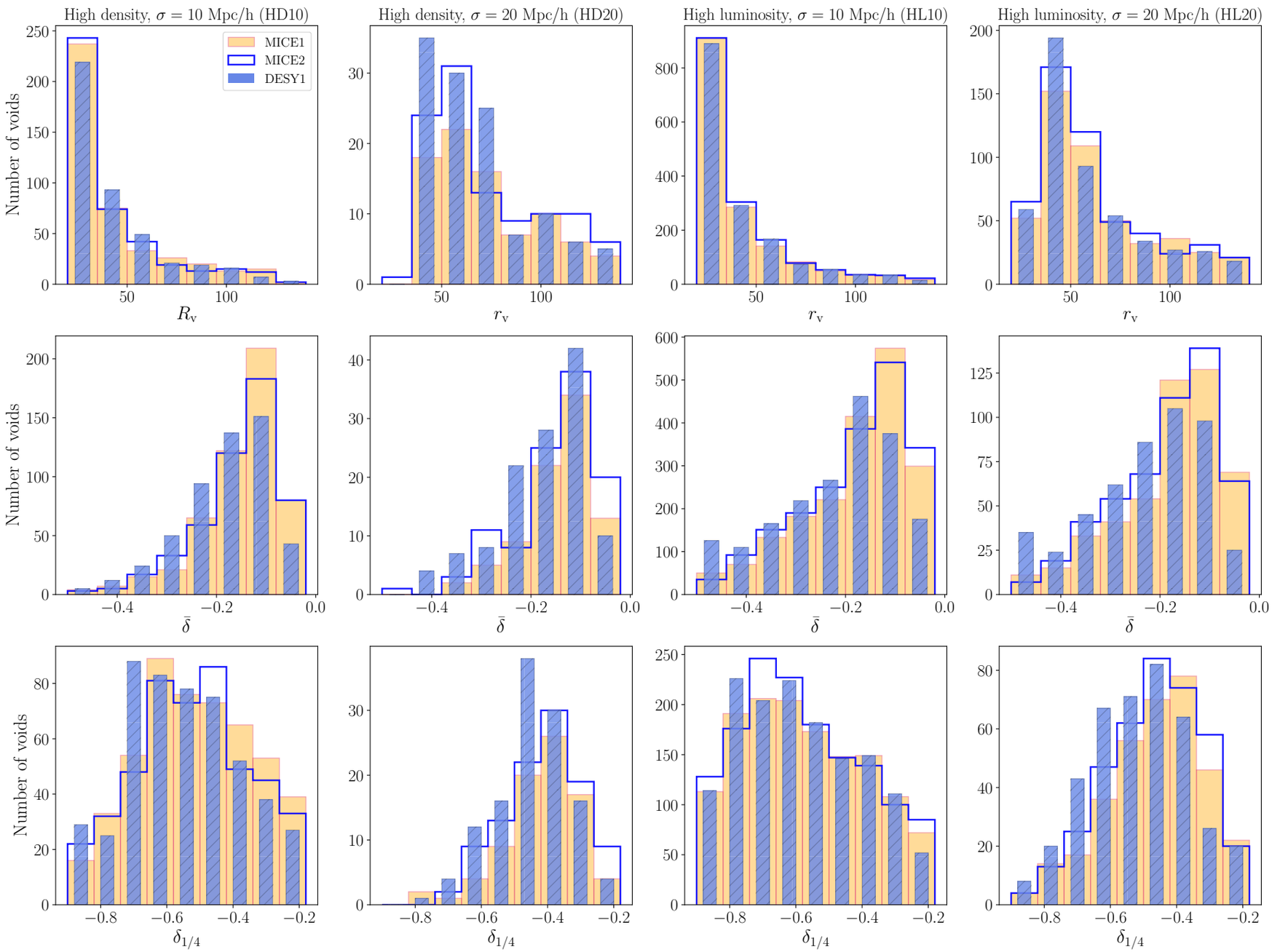

Stacking methodology

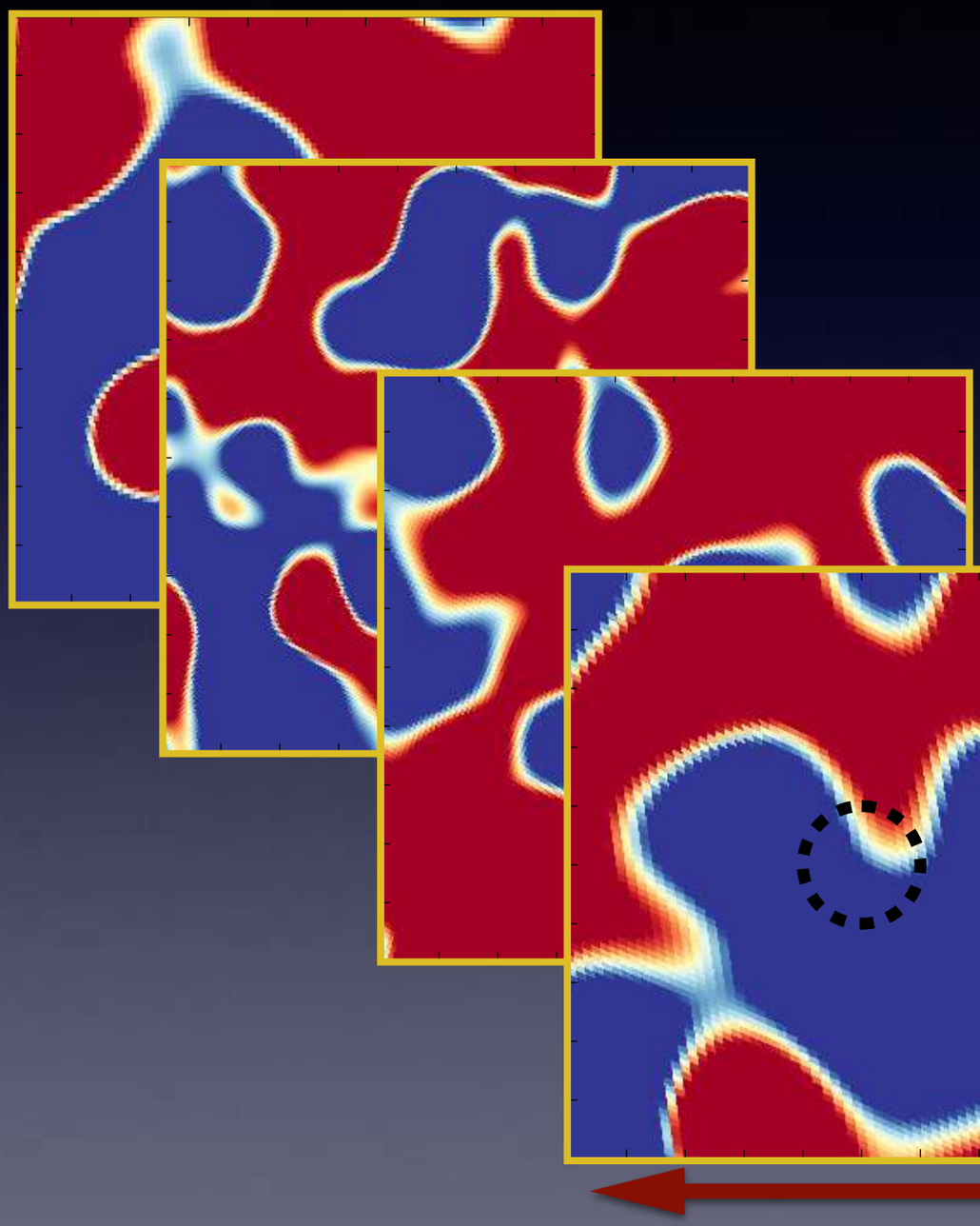

5 times the structure radius

Grannett et al., 2008

- Cutting out patches of the CMB map centered at superstructure position using healpix (Górski et al., 2005).
- Re-scaling the patches given the angular size of the structure.
- Stacking all patches and measuring the average signal in different concentric radius bins around the center.

Stacking methodology

Stacked Healpix image → **CMB convergence profile**

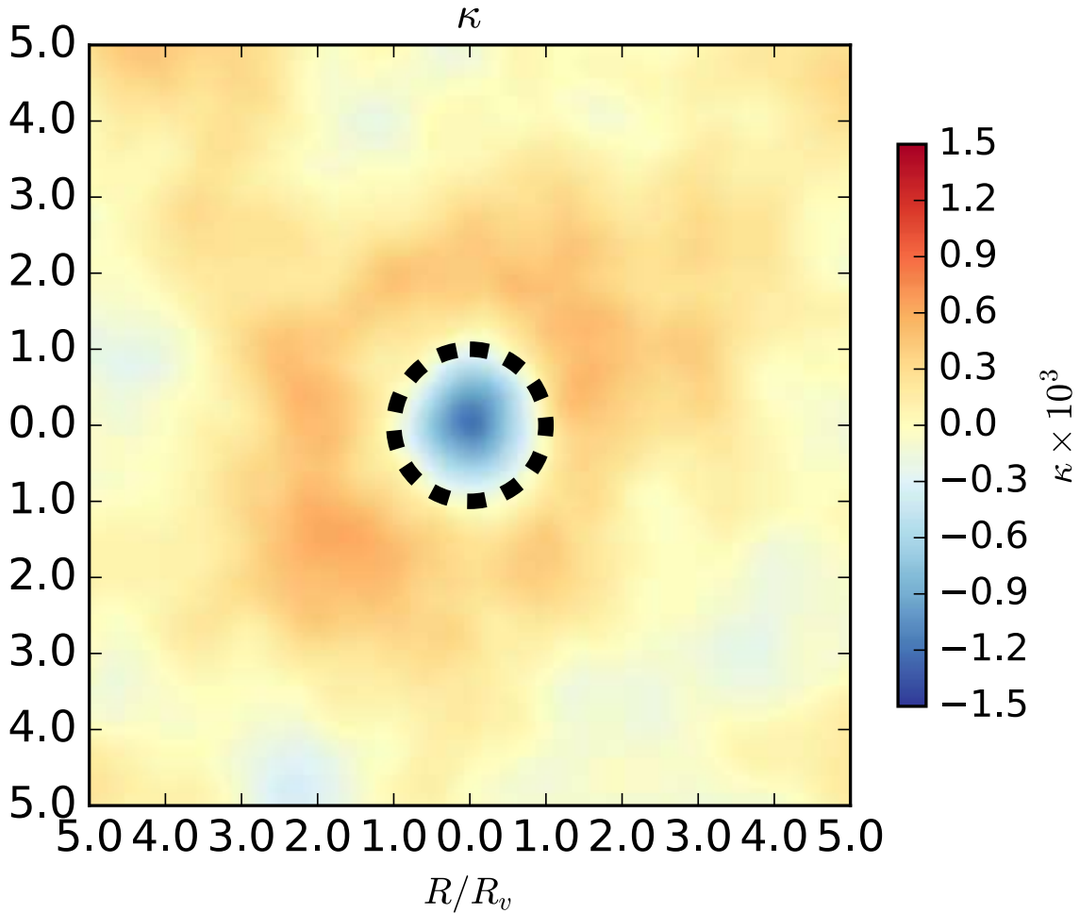

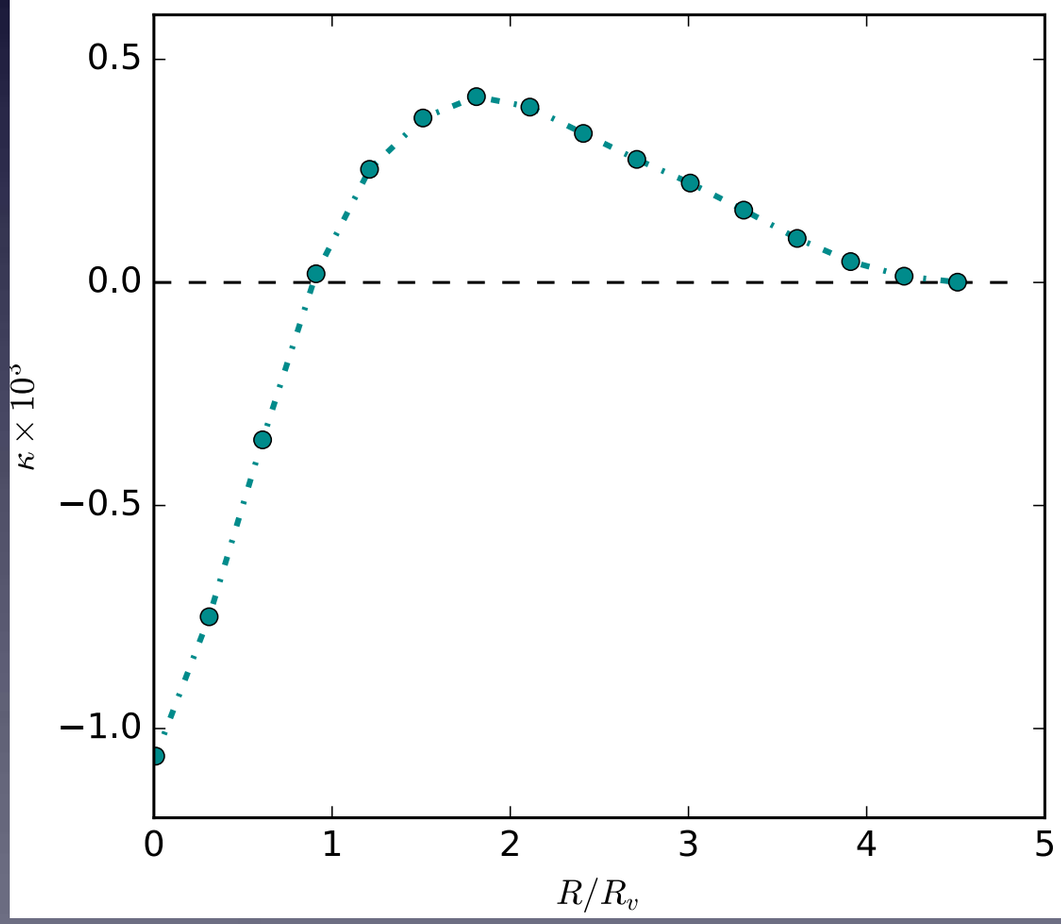

Results

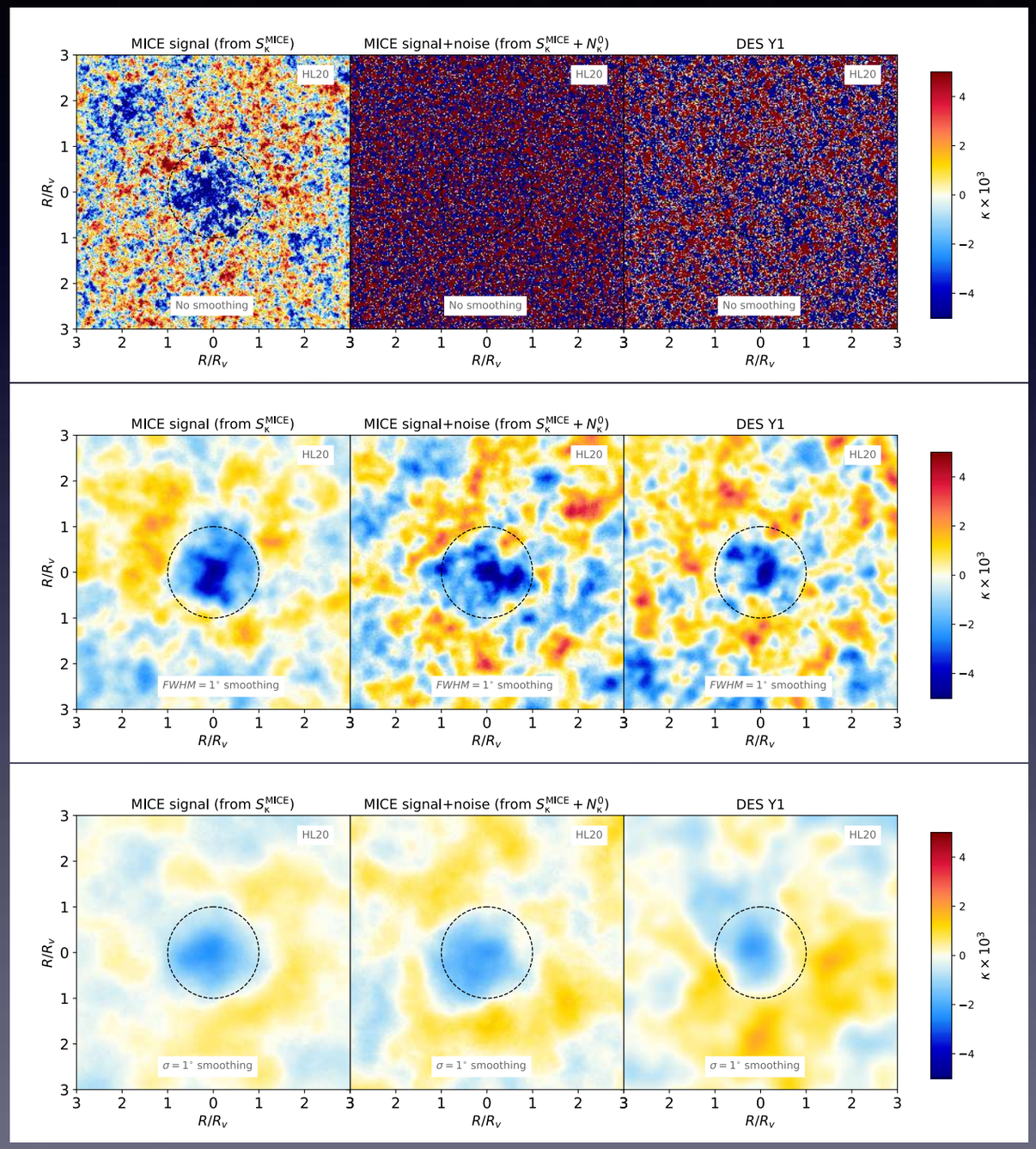
MICE signal (from $S_\kappa^{\rm MICE}$)
MICE signal+noise (from $S_\kappa^{\rm MICE}+N_\kappa^0$)
DES Y1
HL20
No smoothing
$FWHM = 1^\circ$ smoothing
$\sigma = 1^\circ$ smoothing
R/R_v
$\kappa \times 10^3$

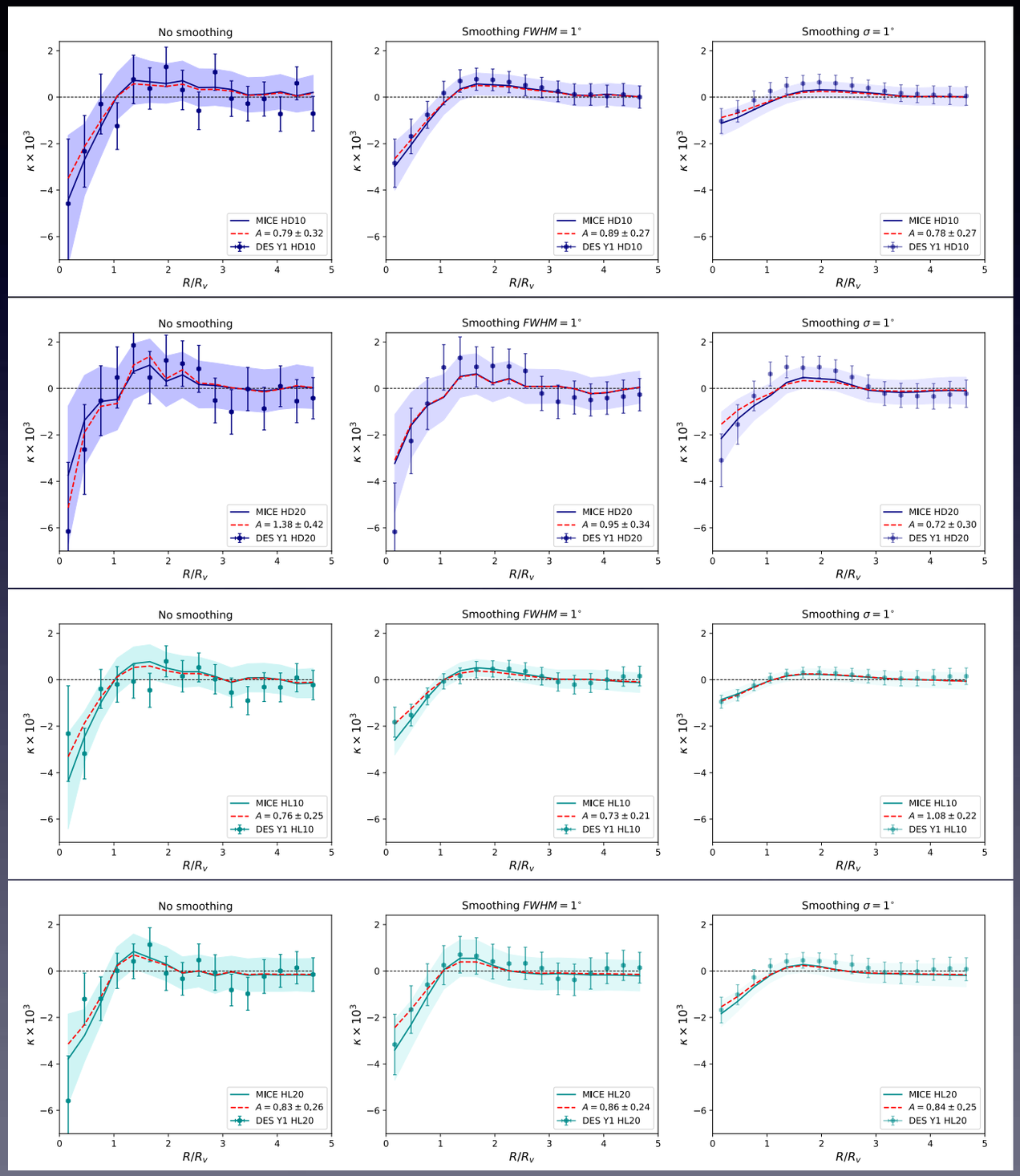
No smoothing
Smoothing $FWHM = 1^\circ$
Smoothing $\sigma = 1^\circ$
MICE HD10
$A = 0.79 \pm 0.32$
$A = 0.89 \pm 0.27$
$A = 0.78 \pm 0.27$
DES Y1 HD10
MICE HD20
$A = 1.38 \pm 0.42$
$A = 0.95 \pm 0.34$
$A = 0.72 \pm 0.30$
DES Y1 HD20
MICE HL10
$A = 0.76 \pm 0.25$
$A = 0.73 \pm 0.21$
$A = 1.08 \pm 0.22$
DES Y1 HL10
MICE HL20
$A = 0.83 \pm 0.26$
$A = 0.86 \pm 0.24$
$A = 0.84 \pm 0.25$
DES Y1 HL20
R/R_v
$\kappa \times 10^3$

Results

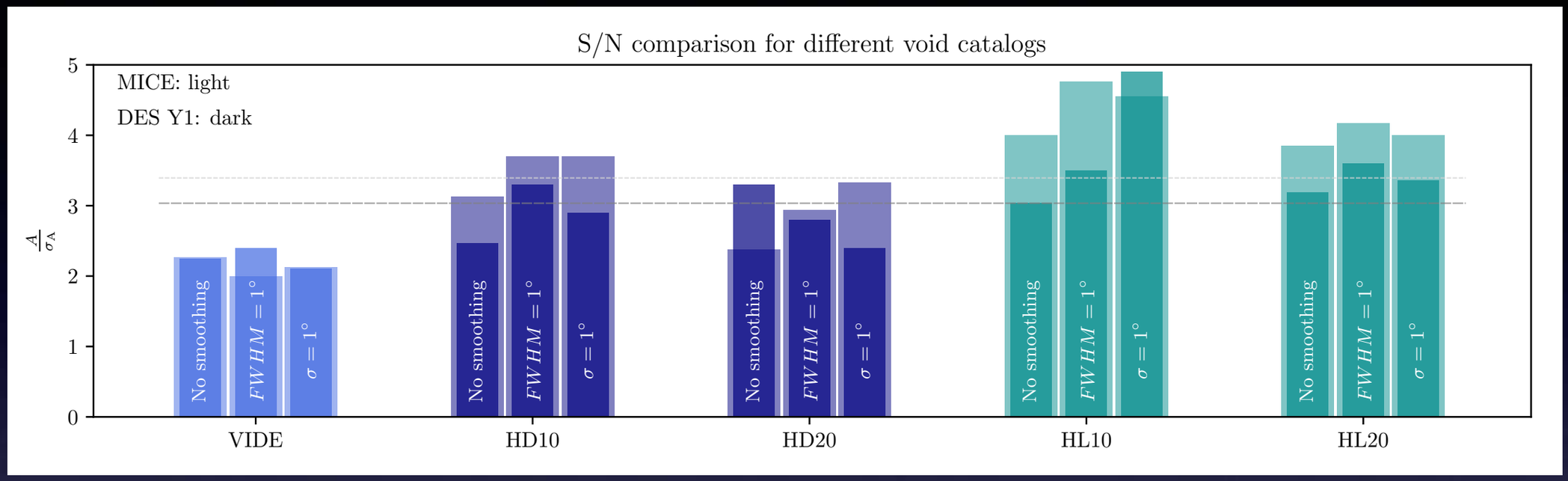

- **3σ significance level**

No smoothing					
Catalogue	VIDE	HD10	HD20	HL10	HL20
MICE	2.27	3.13	2.38	4.00	3.85
DES Y1	2.25	2.47	3.29	3.04	3.36
***FWHM*= 1° smoothing**					
Catalogue	VIDE	HD10	HD20	HL10	HL20
MICE	2.00	3.70	2.94	4.76	4.17
DES Y1	2.42	3.30	2.79	3.48	3.58
σ = 1° smoothing					
Catalogue	VIDE	HD10	HD20	HL10	HL20
MICE	2.13	3.70	3.33	4.55	4.00
DES Y1	2.11	2.89	2.40	4.91	3.19

- We then comprehensively searched for the best combination of parameters that guarantees the best chance to detect a signal with observed DES data. We concluded that the lower tracer density of the higher luminosity *redMaGiC* galaxy catalogue is preferable to achieve a higher signal-to-noise for both 10 Mpc/h and 20 Mpc/h initial Gaussian smoothing.

Conclusions

. DESY1 gave us competitive results in cosmological analysis

- DESY1 have made the stronger cosmic shear signal detection.
- The combined cosmological analysis using DES large scale structure have begin to be statistically strong enough to be competitive with the CMB.
- DESY1 combined with additional probe allowed us to put the tightest constraints today in cosmological parameter namely for LCDM:

$$S_8 = 0.799^{+0.014}_{-0.009} \qquad \Omega_m = 0.301^{+0.006}_{-0.008}$$

- wCDM, no evidence for varying equation of state parameter :

$$w = -1.00^{+0.04}_{-0.05}$$

- Tensions remains looking forward y3/6
- We have now large and precise sample that (will) allows us to use cosmic voids as cosmological probe.
- We robustly detected imprints at the 3σ significance level with most of our analysis choices, reaching *S/N* ≈ 4 in the best predicted measurement configurations using DES Y1 high luminosity *redMaGiC* data.

Unknown systematics in DES data :

The internal consistency of the other DES probes, along with their consistency with external cosmological probes, rule out the possibility that the tension observed with the DES Y1 clusters data is driven by observational systematics affecting the DES data (e.g. photometry or shear calibration).

at least one aspect of our theoretical model is incorrect

Wrong cosmology : tension in Standard model exists…

stacked weak lensing signal as mean cluster mass is incorrect

or

the richness–mass relation and/or selection function is flawed.

Back-up

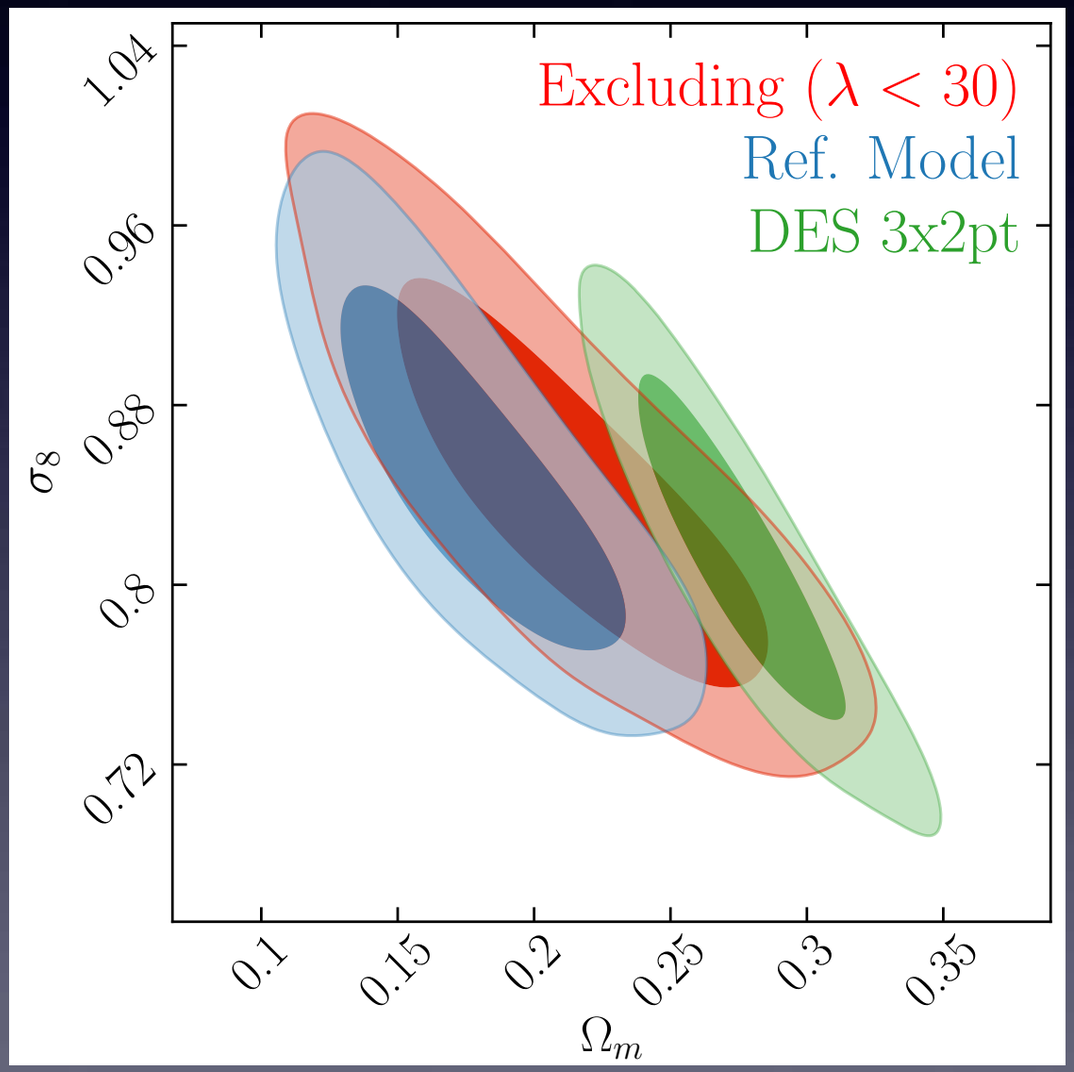
Excluding ($\lambda < 30$)
Ref. Model
DES 3x2pt
1.04
0.96
0.88
0.8
0.72
σ_8
0.1
0.15
0.2
0.25
0.3
0.35
Ω_m